RF-SPUTTERED DEPOSITION OF AlN ON 4H-SiC AND EFFECTS OF ANNEALING ON ELECTRICAL CHARACTERISTICS OF Al-AlN-SiC MIS CAPACITORS

Project Report

submitted by

MEGHABARNA DAS

EE10B065

in partial fulfilment of the requirements for the award of

MASTER OF TECHNOLOGY

and

BACHELOR OF TECHNOLOGY

in

ELECTRICAL ENGINEERING

with specialization in

MICROELECTRONICS AND VLSI

DEPARTMENT OF ELECTRICAL ENGINEERING

INDIAN INSTITUTE OF TECHNOLOGY MADRAS.

MAY 2015

THESIS CERTIFICATE

This is to certify that the thesis titled **RF-SPUTTERED DEPOSITION OF AlN ON 4H-SiC AND EFFECTS OF ANNEALING ON ELECTRICAL CHARACTERISTICS OF Al-AlN-SiC MIS CAPACITORS** submitted by **MEGHABARNA DAS (EE10B065)**, to the Indian Institute of Technology Madras, Chennai for the award of the degrees of **BACHELOR OF TECHNOLOGY AND MASTER OF TECHNOLOGY**, is a bona fide record of the research work done by him under my supervision. The contents of this thesis, in full or in parts, have not been submitted to any other Institute or University for the award of any degree or diploma.

Research Guide
Dr. Nandita DasGupta
Professor
Department of Electrical Engineering
IIT-Madras, 600 036

Place: Chennai
Date: May 2015

ACKNOWLEDGEMENT

I would like to thank my guide Dr. Nandita Dasgupta for inspiring me in the field of VLSI fabrication and compound semiconductors. Being provided with an opportunity to work as a research student under her has been an enriching learning experience. The motivation and support that I received from her is unfathomable. During the course of this project, I not only gained deeper understanding of the field but also felt a sense of strict discipline that is necessary in the field of fabrication being instilled in me.

I would like to thank my seniors Gourab Dutta and Madhup Shukla for training me and supporting me in this project. From training me in fabrication to clearing my doubts, they have been extremely patient with me all throughout. From rectifying every little mistake to teaching me the concepts and principles, they ensured that I learnt well in every step.

I would also like to thank all the staff member of Microelectronics and MEMS Lab, IIT Madras for providing me with all the support needed for completing my project work. Without their support, it would not have been possible to carry out the experiments.

I sincerely thank you all.

Meghabarna Das

ABSTRACT

KEYWORDS: silicon Carbide (SiC), Aluminium Nitride (AlN), High-k dielectric, Metal Insulator Semiconductor(MIS) Capacitor, Post Deposition Anneal (PDA), Post Metalization Anneal (PMA), Rapid Thermal Anneal (RTA)

SiC is a promising semiconductor substrate for high power high temperature devices. It has superior properties like wide bandgap and high thermal conductivity, and conventional fabrication technologies used for Si can be used for SiC as well. With scaling down of device sizes, gate leakage current is becoming a limitation. To overcome those, high-k dielectrics are being implemented as the insulator layer MIS devices. AlN is a suitable high-k dielectric for SiC because of very low lattice mismatch and high thermal conductivity.

The present research work is aimed at developing a metal-insulator-semiconductor device in order to study the electrical characteristics of AlN as an insulating layer with SiC being the semiconductor layer, and Al acting as the gate metal. The technique used for deposition of AlN on SiC carbide was RF-sputtering mechanism using an AlN target. Two types of Post Deposition Annealing techniques were used – Low temperature furnace anneal (400℃) and Rapid thermal Anneal (1000℃). The effects of low temperature PDA for different time durations are studied in Si and the optimum parameters are applied to SiC based MIS capacitors. The combined effects of PDA and PMA are investigated. It also investigates the effects of RTA as a post deposition annealing technique and the effects variations of time and temperatures of RTA are studied. Room temperature electrical characterisations of I-V and C-V have been carried out under dark conditions. The leakage current densities, breakdown fields, interface state density and charge concentrations have been estimated. It therefore investigates the viability of AlN as an insulating layer in acting as a MIS capacitor. The comparison, advantages and disadvantages of each technique applied have been discussed at the end of the study.

TABLE OF CONTENTS

LIST OF TABLES

LIST OF FIGURES

ABBREVIATIONS

AlN	Aluminium Nitride
C-V	Capacitance-Voltage
GaN	Gallium Nitride
High-k	Higher Dielectric Constant
IGBT	Insulated Gate Bipolar Transistor
ITRS	International Technology Roadmap for Semiconductors
I-V	Current-Voltage
J-E	Current Density-Electric Field
MOS	Metal Oxide Semiconductor
MIS	Metal Insulator Semiconductor
MOSFET	Metal Oxide Semiconductor /field Effect Transistors
PDA	Post Deposition Anneal
PMA	Post Metalization Anneal
RCA	Radio Corporation of America
RF	Radio Frequency
RTA	Rapid Thermal Anneal
SiC	Silicon Carbide

NOTATIONS

E_c	Critical Breakdown Field strength
V_G	Gate Voltage
k	Dielectric constant
t_{ox}	Oxide/Insulator thickness
E_G	Gate Electric Field
D_{it}	Density of Interface States
I_G	Gate Current
J_G	Leakage Current Density
Q_f	Fixed Insulator Charge
ΔE_c	Conduction Band Offset
μ	Mobility of carriers
ε_s	Semiconductor permittivity
σ_T	Thermal Conductivity

CHAPTER 1

INTRODUCTION

1.1 Introduction to SiC and High-k dielectrics

The semiconductor industry has benefitted immensely with the discovery of Silicon's effectiveness as a semiconductor. Over the years, technology for fabrication of devices has developed and advanced around Silicon since it favours in terms of higher availability. For the development of devices, the natural oxide of Si, SiO_2, is the widely favoured dielectric because of its compatibility with Si and the reliability of the oxide layer.

In current times, there has been a global aim to move towards energy efficient electronics technology so as to reduce the overall power consumption. In most areas such as industrial, manufacturing, consumer, transportation, medical, power electronics systems have a key role to play in determining the impact on economy and revenues. Thus the aim is to make power electronic systems as efficient as possible. In power electronic systems, several types of solid state power semiconductor devices are used for a variety of applications. Most power electronic devices such as thyristors, IGBTs, etc. require high voltage rating and high current handling capacities and a wide safe operating area for them to be successful in the desired objective [1].

In the field of power semiconductor devices, silicon has limitations because of lack of switching and thermal robustness. Because of limited switching capacities, there are significant switching losses Si based devices. In addition, there is requirement of filters to reduce noise which again is rated for high power. Moreover, to maintain the operating temperature large sinks and cooling mechanisms are needed along with these devices. As a result, silicon has thus reached its theoretical limit in its use in power semiconductor devices [2].

This is where the importance of wide bandgap materials comes into picture. The very fact that these materials have a wider bandgap allow them to withstand much higher temperatures and voltages compared to silicon based devices. Materials such as gallium nitride (GaN),

Silicon Carbide (SiC), diamond have become major game players in power semiconductor devices because of the promise they showed. This is owing to their superior characteristics like high bandgap, large thermal conductivity, high critical breakdown field strength and high saturation velocity. These further result in reduction in weight of devices and improvement in efficiency. The comparison between the parameters of Si and wide bandgap devices are presented in Table 1.1.1 [26].

Table 1.1.1: Comparison of parameters of Si and Wide Bandgap Materials

Semiconductor Material	Bandgap (eV) Direct (D) Indirect (I)	Electron Mobility, μ_e $(\frac{cm^2}{Vs})$	Hole Mobility, μ_h $(\frac{cm^2}{Vs})$	Density $(\frac{g}{cm^3})$	Breakdown Field, E_c $(\frac{V}{cm})$	Thermal conductivity, σ_T $(\frac{W}{m.\kappa})$	Relative dielectric Constant, ε_s
Si	1.12, I	1400	450	2.33	300,000	130	11.9
GaN	3.44, D	900	10	6.1	300,000	110	9.5
SiC (3C, β)	2.36, I	300	10	3.17	1,300,000	700	9.72
SiC (6H, α)	2.86, I	330	75	3.21	2,400,000	700	9.66
SiC (4H, α)	3.25, I	700	115	3.19	3,180,000	700	9.7

Silicon carbide has a higher thermal conductivity and SiC power devices have a lower junction-to-case thermal resistance which assures that device temperature increase is slower. Moreover, reports show that operation at temperatures as high as 600°C is feasible for SiC, whereas Si cannot operate beyond the junction temperature of 200℃ [6]. Hence the need for external cooling systems and special packaging for SiC based devices reduces compared to their silicon counterparts. SiC has higher saturated drift velocity ($2 \times 10^7\ cm/s$) allowing operation at higher cut-off frequencies as well.

Although GaN and SiC show similar improvements over Si, the advantage with SiC lies in the fact that technologies associated with SiC are at a more advanced stage [3]. It has similarities with silicon in since they have the same native oxide, silicon dioxide. As a result of which, the state-of-the-art technologies available for silicon can be borrowed and used for silicon carbide as well.

With the scaling down of device size over the years with technology scaling, the number of devices on a chip has increased giving high package density, and also high electronics circuit speed and lesser power dissipation [4]. This was in accordance with 'Moore's Law' which predicted that the number of transistors that could be placed on an integrated circuit would double every two years [5]. This has led to development of 'roadmap' by ITRS (International Technology Roadmap for Semiconductor) with is updated annually specifying the desired scaling down targets to be met by technological advancements in fabrication [6].

But with the reduction in device sizes, the leakage current has increased. This has led to increased power consumption. As a result, the search for dielectrics with higher dielectric constant has been on and thus the advent of $high-\kappa$ dielectrics has been of utmost importance.

The term high-k refers to the high dielectric constant. To overcome the limitations of SiO_2, it is straightforward to use a high-k dielectric material as the insulator layer. They meet the b=necessary requirements of being electrically thin and physically thick. Although a larger capacitance and higher mobility requirements can be met with high-k dielectrics, the quality of interface between the semiconductor and the insulator is of high importance. If the interface is not of good quality, it can be the reason of traps which can degrade the performance of the devices It is therefore necessary to investigate technologies to reduce the leakage currents in the devices.

1.2 Motivation of this research work

We have seen the rising importance of SiC as a semiconductor substrate in the previous section 1.1. Also, the necessity of high-k dielectrics in the current scenario has been highlighted. AlN is a high-k dielectric substance with a large band gap and high thermal conductivity. It also has a small thermal expansion coefficient. Also, under ambient conditions, it crystallizes in the hexagonal wurzite structure [7]. It has a close lattice match with SiC which allows the growth of high-quality epitaxial layers on SiC. The mismatch reported is around 0.9% only. Therefore it is one of the suitable dielectrics that can be considered for SiC based devices. Till now, various deposition techniques of AlN on SiC have been tried [8] [9] [10] [11], among which sputtering is a popular technique. This study aims to find the electrical characteristics of such Al-AlN-SiC MIS capacitors made by RF sputtering and to explore different annealing and their effects on such devices as that.

1.3 Objectives and Scope of this work

The objective and scope of the current work is given as

- To optimise the parameters of RF sputtered deposition of AlN on Si and investigate effects of gas flow rate ratio
- To study the effects of variations of post deposition annealing time for AlN on Si
- To study the effects of post metalization anneal for AlN on SiTo fabricate MIS capacitors on SiC substrate using the optimised parameters observed
- To implement and study the effect of low temperature furnace based post deposition anneal on the electrical characteristics of Al-AlN-SiC MIS capacitors
- To study the effects of low temperature furnace based post metalization anneal on the electrical characteristics of Al-AlN-SiC MIS capacitors and also to investigate the combined effects post deposition anneal and post metalization anneal
- To investigate the effects of variations of rapid thermal annealing on the electrical characteristics of Al-AlN-SiC MIS capacitors

1.4 Organization of this the thesis

This thesis is organized into six chapters. In the first chapter, a background SiC and high-k dielectrics and their importance is presented, following which the motivation and objectives of this study is given. The second chapter gives a brief literature survey of structures and properties of SiC and AlN. A description of RF sputtering basics and the reasons for using this deposition technique in this study is presented which also includes a schematic description of the RF sputtering system used in our lab for the present work. Following this, rapid thermal annealing and its usages have been reviewed. The third chapter deals with the optimization of deposition parameters for fabrication of Al-AlN-Si MIS capacitors. The fabrication of Al-AlN-SiC MIS capacitors and the effects of low temperature furnace annealing are discussed. The fifth chapter presents the investigation on rapid thermal annealing as a post deposition annealing technique for Al-AlN-SiC MIS capacitors. The results are summarized and conclusions are presented in chapter six.

CHAPTER 2

LITERATURE SURVEY

2.1 Silicon Carbide Structure and Properties

Silicon Carbide has a tetragonal structure of four carbons atoms with a silicon atom in the centre and each carbon atom is surrounded by four silicon atoms as well. The atoms are covalently bonded to each other with the silicon-carbon bond and carbon-carbon bond being equally thermodynamically stable.

Two different types of SiC polytypes are found. Polytype refers to any number if forms of a crystalline substance which differ only in one of the dimensions of the unit cell (online). The basic two crystalline structures found are cubic polytype or β-SiC and non-cubic polytype (hexagonal and rhombohedral) polytype known as α-SiC. The most common polytypes of SiC presently being developed for electronics are 3C-SiC, 4H-SiC, and 6H-SiC. The different polytypes of SiC are actually composed of different stacking sequences of Si–C bilayers (also called Si–C double layers). For example, in 3C-SiC, the letter "C" refers to the cubic structure and the number "3" refers to the number of double-atomic layers in one repeating unit. Each atom within a bilayer has three covalent chemical bonds with other atoms in the same (its own) bilayer, and only one bond to an atom in an adjacent bilayer [12]. The figures shown below represent the structures of different polytypes mentioned. Fig 2.1.2.b. shows that 4H-SiC has four Si–C bilayers to define the unit cell repeat distance along the c-axis stacking direction. (The c-axis denotes the direction normal to the Si–C double-atomic layers (Fig2.1.1.a)).

The different polytypes exhibit different stacking arrangements. As a result, the electrical and optical properties vary among them. The bandgap is different and also electron mobility, hole mobility, breakdown field and thermal conductivity also vary significantly (Table1.1.1). It is observed that the indirect bandgap increases with increasing hexagonality of the polytype. The 4H-SiC polytype is generally preferred to the other to polytypes because of higher mobility and thermal conductivity.

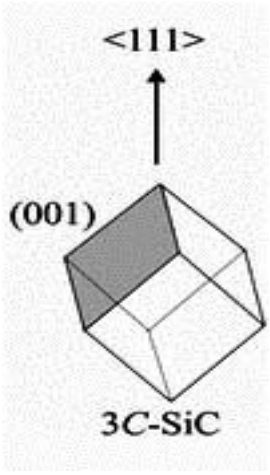

Fig 2.1.1.a. Crystal Axis of cubic SiC

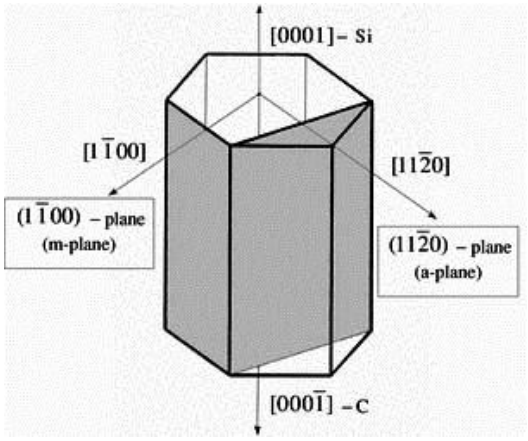

Fig 2.1.1.b. Crystal Axis of hexagonal SiC

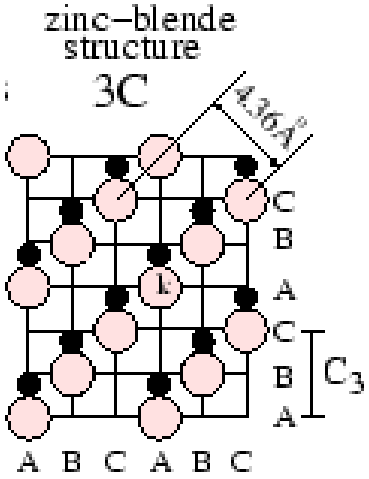

Fig2.1.2.2a. 3C-Sic Polytype

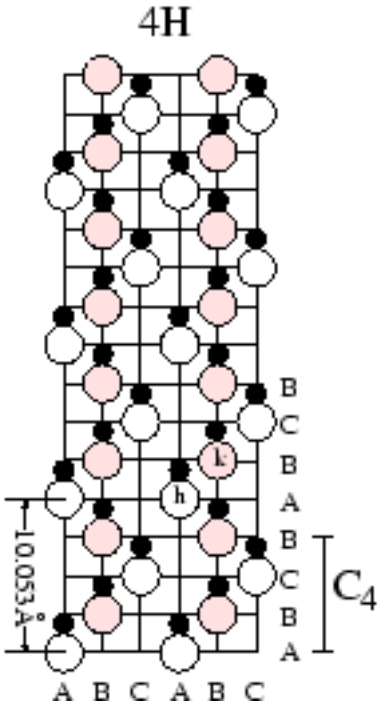

Fig2.1.2.b. 4H-Sic Polytype

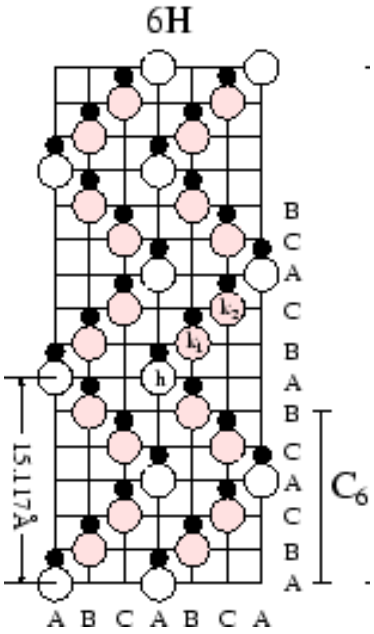

Fig2.1.2.c. 6H-Sic Polytype

The comparison of 4H-SiC with silicon shows improved thermal stability (atleast three times more) which makes it suitable and reliable choice for high-temperature operations. Thus the expected benefits of lower power losses, improved efficiency, lesser heat generation, easier cooling, smaller size that are promised by wide bandgap semiconductors can be obtained using 4H-SiC. Overall, there can be reduction in costs associated with power electronic devices.

2.2 Aluminium Nitride Structure and Properties

Aluminium nitride is characterised by a high bandgap (around 6.015eV). This makes it suitable for high temperature electronics. The melting temperature of AlN is approximately 3000°C which is the reason for its high temperature stability. It also has elastic stiffness and good thermal conductivity [13].

There are two types of structures of AlN- zinc-blend and wurzite. Wurzite AlN (w-AlN) has a direct bandgap. This is a mostly covalent material. This is the form in which AlN crystallizes. The structure consists of hexagonal close packing of the anions with the cations occupying half the tetrahedral sites. The properties of AlN are listed in the Table 2.2.1.

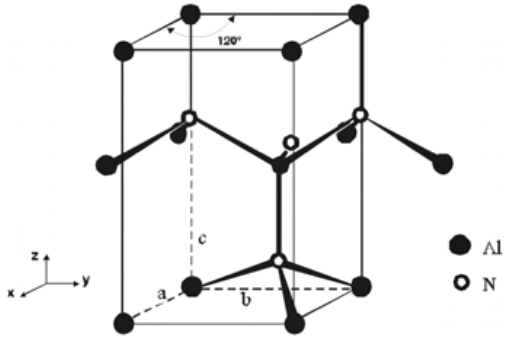

Fig2.2.1 Structure of Aluminium Nitride (online)

Table 2.2.1: Properties of AlN

Melting point	3273 K
Thermal conductivity	210-285 $(\frac{W}{m.\kappa})$
Thermal expansion coefficient	$4.14 - 5.27 \times 10^{-6} K^{-1}$
Conductivity	$10^{-11} - 10^{-13} \Omega^{-1} cm^{-1}$
Dielectric constant	9-10.42

From the above parameters, we can clearly see that AlN is highly stable thermally. Its thermal expansion coefficient matches that of Si. The resistivity is high and most importantly, it has a high dielectric constant, almost 2.5 times of that of SiO_2, which has a dielectric constant of 3.9. All of these parameters make AlN an attractive choice as a high-κ for MIS type semiconductor devices in the role of gate dielectric.

Over the years, AlN has found its use into various fields. In compound semiconductor devices, AlN acts as a buffer layer and improves adhesion between GaN and substrates (more in the case of Si and SiC as the substrate). In the area of integrated circuits, it finds its use as a substrate and packaging material. Moreover, its usage has been considered in variety of fusion reactors, magnetic insulation and RF windows [14]. AlN also has blue and a UV light emitting property, which means it can integrate the fields of optoelectronics with silicon microelectronics. It can be used in light-emitting diodes, laser diodes, field emission display. This is based on the effectiveness of AlN as the insulator layer in metal-insulator-semiconductor structure [15]. It specially shows potential for optoelectronic devices operating at sorter wavelengths as well as for high temperature and high power devices [16]. Also, its use is found in acoustic-electronic devices such as surface acoustic wave and bulk acoustic wave devices.

For all these reasons, Aluminium Nitride seems to be a promising dielectric material for being suitably used in high power high temperature devices. Hence, this study aims to investigate the viability of Al-AlN-SiC MIS capacitors.

2.3 Radio Frequency Sputtering

Sputtering is a type of deposition technique where target of the substance to be deposited is bombarded with high energy ions in order to break the bonds of the atoms holding the atoms onto the solid, thus dislodging them from their location. The target is bombarded with high energy Ar+ ions, and the knocked off atoms from the target travel until they strike the wafer's surface, where they deposit to form the desired layer [17].

The basic process that occurs in an RF sputtering chamber is that ionic plasma is created by applying a high voltage to a glow tube. Plasma is nothing but ionised gas which is created by breaking down gas molecules by applying a certain voltage. The target is as the cathode.

Generally, cylindrical shapes of cathodes are preferred. The atoms in the target are ejected from the cathode by energy and momentum. The other electrode is called anode, which is grounded so that the ratio of the target to anode area is significantly reduced. The inert gas to create the high energy ions should be of the right size with their atomic weight being close to the atomic weight of the target atoms. Argon is generally preferred as the inert gas so as to prevent any kind of reaction between the sputtered atoms and the sputtering gas. A suitable pressure needs to be created in the chamber, and the right cathode voltage must be applied so that the ions have the right amount of energy for sputtering [18]. The ions are accelerated towards the target by utilizing electric field.

In case of reactive sputtering, another reactive gas in controlled amount is introduced into the chamber to produce the required material composition. The reason this technique is so popular is that high coating and controlled deposition rates can be achieved with this technique [19]. For the purpose of sputtering, a high purity target usually larger than the size of the wafer is required for uniform deposition. In this technique, a better control over material composition is possible. Also, it has the advantage of low-temperature deposition, ease of synthesis. It is also less expensive and produces good quality films with a fairly smooth surface.

RF sputtering is particularly used for deposition of insulators and dielectrics. This is because in during sputtering, when the plasma ions strike the target, the electrical charge is neutralised and they return to the process as atoms. This causes a build-up of a huge positive charge on the cathode (i.e., target surface) and this might lead to the need of around need 10^{12} volts to sputter insulators. This might eventually lead to the repulsion of the high energy ions from the sputtering surface and as a result the deposition rate becomes inconveniently slow. For this reason, a periodic reversal of polarity is needed to attract enough electrons from the plasma to neutralise the surface charge [20]. This is done by applying radio-frequency (RF) voltage on the target assembly. This technique is hence known as RF sputtering.

The RF sputtering system used in this study is “Hind High Vacuum’s RF Sputtering Unit”. A schematic diagram of the RF sputtering assembly used in this study is given in Fig. 2.3.1.

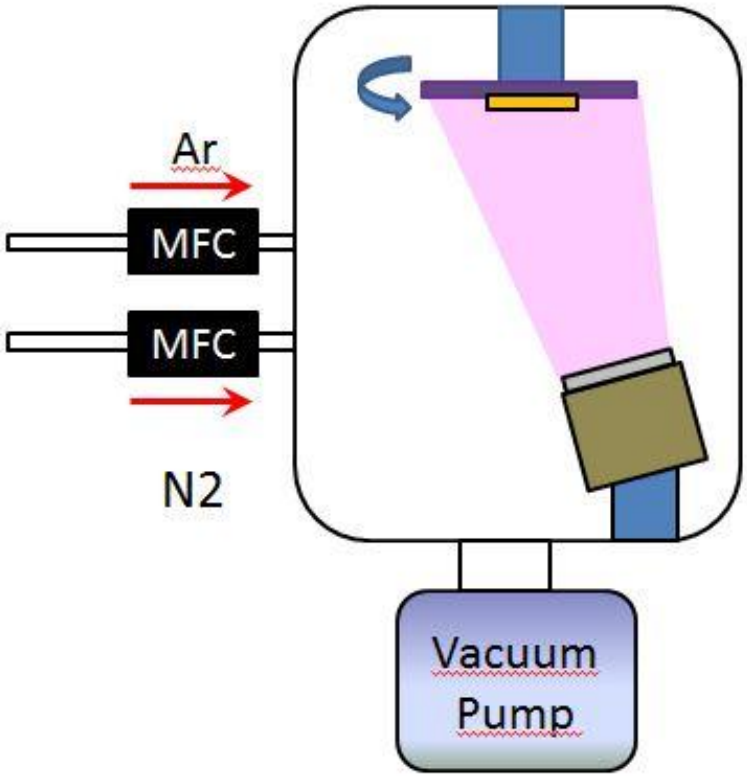

Fig 2.3.1: Schematic of RF Sputtering system used in the study

For the deposition of AlN on Si or SiC, a controlled mechanism is needed and the purity of the sputtering atmosphere needs to be ensured. The deposition parameters like sputtering temperature, pressure, power and wafer to target distance need to be optimized to get the best results. It has been reported that in case of DC sputtering systems, even if some traces of impurity is present in the sputtering chamber, the surface of the Al or AlN target being used becomes contaminated and target poisoning takes place [21]. So, RF sputtering is preferred.

Using RF sputtering mechanism, epitaxially grown ALN on SiC with a good c-axis orientation was reported [9]. In those cases, a good interface of AlN-SiC was achieved which resulted in very low leakage currents in the MIS capacitors fabricated. It has also been reported that the AlN films deposited using RF sputtering had the preferred wurzite structure with a uniform and smooth surface morphology.

2.4 Rapid Thermal Anneal

Rapid Thermal Annealing is a subset of rapid thermal processing. In RTA, the temperature inside the annealing chamber is ramped up to extremely high temperature in a matter of seconds or less. The wafers are subjected to the set temperature of a few seconds, and the temperature is then ramped down. This kind of processing is used to affect the electrical properties of the wafer and only a single wafer can be processed at a given time. Rapid thermal anneals are performed by equipment that heats a single wafer at a time using lamp based heating that a wafer is brought near. Unlike furnace anneals they are short in duration, processing each wafer in several minutes [22].

The effects of RTA on AlN layer have been studied. Very low leakage current densities of $10^{-9} A/cm^2$ have been reported at an electric field of $2\ MV/cm$ for RTA usage for a film thickness of 53nm [9]. The film has been studied to show a higher c-axis orientation and better morphology. Hence, for AlN deposition on SiC, RTA can be used to obtain low leakage current densities.

CHAPTER 3

RF Sputtered Deposition of AlN on Si for Optimization of Parameters

3.1 Introduction

The experiments on RF-sputtered AlN on Si are done prior to the experiments with silicon-carbide as a substrate to check the effectiveness and bulk characteristics of AlN as a gate dielectric. These series of experiments are aimed at optimizing the entire experimental procedure to arrive at the best set of parameters for the deposition process. The parameters which give optimum dielectric characteristics of AlN as a gate dielectric would be set as the parameters the experiments henceforth.

3.2 Experiment Details of RF-Sputtered AlN on Si – Effects of Nitrogen Flow rate during Deposition

The crystallinity and morphology of the deposited AlN is influenced by the ratio of Ar/N_2 gases, and also the temperature of deposition, as they determine the kinetics of sputtered atoms that arrive at the surface of the substrate [23]. As mentioned earlier, the inert argon gas produces argon ions in plasma due to sputtering power which then go and strike the target and produce AlN atoms. In cases of reactive RF sputtering, an Al target is used instead of an AlN target, and Al atoms are produced instead. In that case, Al atoms react with nitrogen and form the required AlN compound. So the ratio and flow rate of nitrogen gas plays an important role in determining the quality of the layer obtained. It has been reported that in case of reactive RF sputtering using Al target, higher nitrogen flow rate and lower argon flow rate gives more time interval for the arrival of Al species at the surface. Because of that, the Al atoms get sufficient time to react with N_2 which increases the probability of better Al-N bond formation and get more time to adjust themselves on the substrate. A lower N_2/Ar ratio results in poorly bonded compounds and rougher surface. Hence a higher gas flow rate of N_2 is desired compared to Ar [21].

In case of AlN target, study of the effects of N_2 gas flow rate while maintaining a constant gas flow rate for argon was necessary for the laboratory equipment set-up and conditions.

The required AlN compound was already available in the form of a high purity target. So the experiments were done to check the differences in electrical characteristics obtained in the resulting devices. The gas flow ratio of N_2/Ar which gave the best results would be set as parameters for all other experiments.

The experiments were carried out on p-type Si substrate of 1-10Ω resistivity. The samples were cleaned and degreased in organic solvents followed by piranha cleaning and dilute Hydrofluoric acid (dil. HF) dip for few seconds. Then they were cleaned in nitric acid and again subjected to dil. HF dip. After each step, the samples were thoroughly rinsed in de-ionised water and blow-dried in N_2 to make sure the native oxide in Si substrate is removed completely.

Immediately after cleaning, the samples were loaded into the RF-sputtering system. The target was of AlN with *2 inch* diameter and of *99.5% purity*. The system chamber was evacuated using a turbo pump until a base pressure of less than $4.5 \times 10^{-7}\ mBar$ was reached. High purity argon was then introduced into the chamber following which the optimum deposition pressure of $1.0 - 1.5 \times 10^{-2} mBar$ was maintained. Nitrogen gas of high purity was then introduced into the chamber. The target was pre-sputtered for 10 minutes prior to deposition with a closed shutter to remove any oxides on the surface. The shutter was then opened and AlN was deposited on Si substrates. The details of sputtering parameters are summarized in Table 3.21.

Table 3.2.1: Initial RF sputtering Parameters

Substrate Temperature	Room Temperature
RF Power	100W
Argon Flow Rate	20sccm
Deposition Time	20mins
Deposition Pressure	$1.0 - 1.5 \times 10^{-2} mBar$

The nitrogen flow rate was varied as 10sccm, 20sccm and 30sccm.

Following deposition, the samples were for Al metal deposition to form the gate metal. It was then patterned to form MOS capacitors of diameter$200\mu m$. Following this, the back-surface of the substrate was given buffered hydrofluoric acid (BHF) dip in order to remove the native back oxide and Al was deposited on the entire back surface to serve as Ohmic contact. Current-voltage (I-V) measurements and high frequency (1 MHz) capacitance-voltage (C-V)

measurements were carried out in dark conditions at room temperature using Agilent's B1500A and Cascade Microtech 1100 probe station. The resulting I-V and C-V plots were observed.

3.3 Results of RF-Sputtered AlN on Si – Effects of Nitrogen Flow rate during Deposition

3.3.1 Thickness

The thickness of AlN film deposited was measured to be around 9-10nm in case of nitrogen flow rates of 10sccm and 20 sccm. In case of 30sccm N_2 flow rate the thickness was measured to be 11nm. All other deposition conditions were maintained to be the same. Hence, not much difference in thickness was obtained in these different cases.

3.3.2 Current-Voltage Characteristics

Fig. 3.3.2.1 shows a comparison between the current-voltage characteristics of the three cases of N_2 flow rates. It can be seen that the leakage current decreases with increase in flow rate of N_2 as compared to Argon. This can be attributed to better surface texture of smaller grain size, smoother, homogeneous and dense granular microstructures has been observed at higher concentrations of nitrogen [14]. Thus, this is consistent with available literature.

The best results are obtained in the case where the flow rate parameters are: Ar= 20 sccm, N_2 = 30sccm.

The Current Density vs Electric Field (J-V) curve is plotted below in Fig. 3.3.2.2. The thicknesses of the devices obtained in these cases and the area of each device with respect to $200\mu m$ diameter which is $3.14 \times 10^{-4} cm^2$ and the thicknesses obtained are $10nm$ for 10sccm, $10nm$ for 20sccm and $11nm$ for 30sccm.

The results obtained are in accordance with those obtained in literature [16]. The results are summarised in Table 3.3.2.1.

Table 3.3.2.1: Results of Flow Rate Optimization

Time of Deposition	N2 Flow Rate	t_{ox}	$J_{leakage}$ at $-2\,MV/cm$
20mins	10sccm	10nm	6.305×10^{-6}
20mins	20sccm	10nm	2.248×10^{-7}
20mins	30sccm	11nm	2.500×10^{-7}

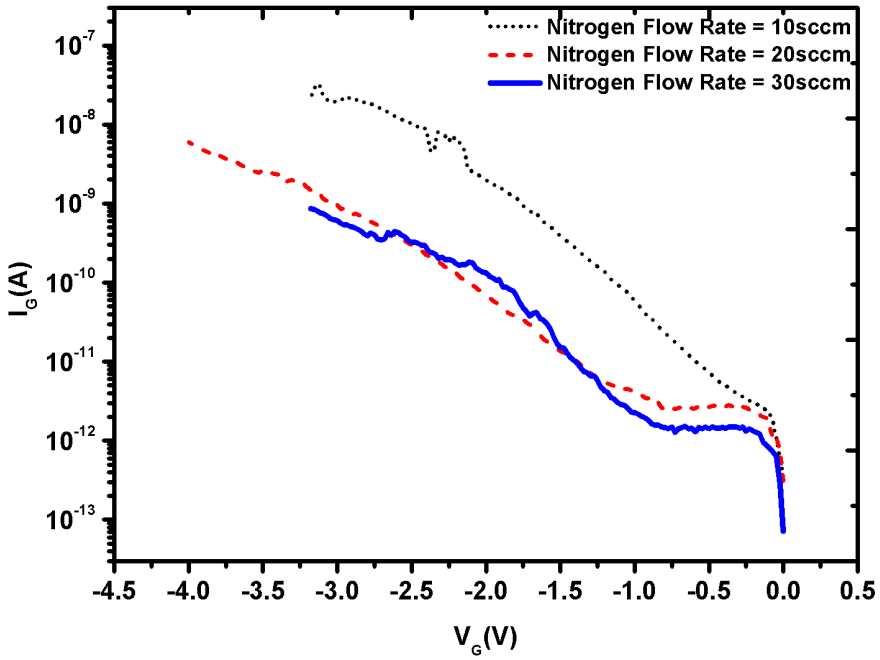

Fig. 3.3.2.1 Plot of current vs voltage for AlN deposited at different N2 flow rates (10 sccm, 20sccm and 30sccm)

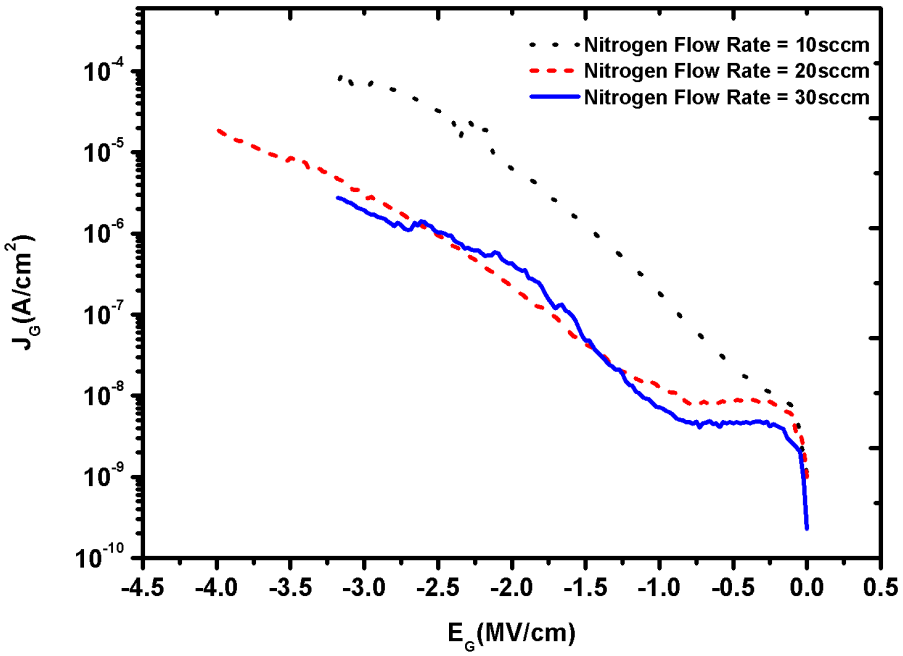

Fig. 3.3.2.2 Plot of current density vs electric field for AlN deposited at different N2 flow rates (10 sccm, 20sccm and 30sccm)

3.3.3 Capacitance-Voltage Characteristics

The capacitance vs. voltage curves were measured at a high frequency of 1MHz. Fig 3.3.3.1 shows the results obtained for different flow rates of N_2 gas. The C-V curves do not show proper saturation of the capacitance in accumulation, and this could not be obtained because of the low breakdown field of the deposited AlN layer. Using the value of the thickness of the AlN layer obtained from ellipsometer measurements, and assuming the value of highest value of capacitance obtained as the accumulation capacitance. These curves are single sweep curves, show hysteresis information could not be obtained from them.

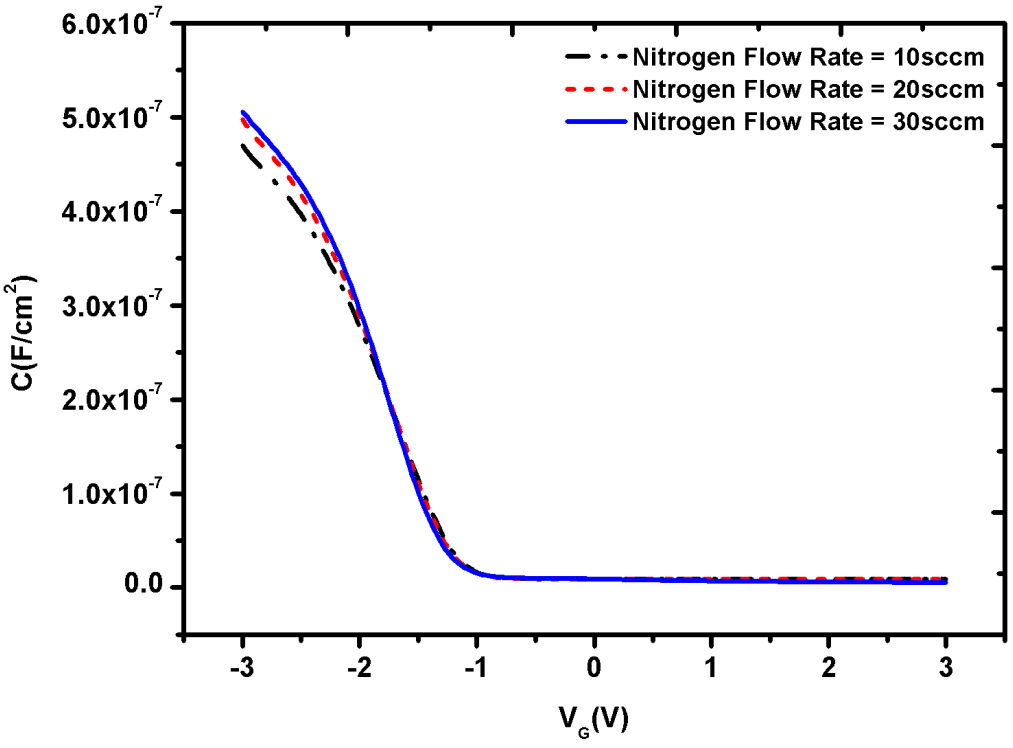

Fig. 3.3.3.1 Plot of capacitance per unit area vs voltage for AlN deposited at different N2 flow rates (10 sccm, 20sccm and 30sccm)

The capacitance did not reach saturation in the above cases and the leakage current isn't optimum. Moreover, the breakdown field is low. The probable reason could be that many of the atoms might not have occupied lattice sites. These might give rise to strain and lead to the formation of voids [14]. For these reasons, post metallization anneal is tried.

3.4 Experiment Details of RF-Sputtered AlN on Si – Effects of Nitrogen Flow rate during Deposition with Post Metal Anneal

To improve the leakage current and to improve the breakdown voltage, post-metalization anneal (PMA) was done. The temperature of the furnace was ramped up to 400℃ with the nitrogen flow rate maintained between 70 and 80 litre/hr. The samples were loaded into the annealing furnace with a nitrogen flow rate of 120 litre/hr. They were then annealed in full nitrogen ambient at 400℃ for 15 mins. The samples were then taken out of the furnace and the temperature of the furnace was ramped down.

Current-voltage (I-V) measurements and high frequency (1 MHz) capacitance-voltage (C-V) measurements were carried out in dark conditions at room temperature using Agilent's B1500A and Agilent's B1500A and Cascade Microtech 1100 probe station. The resulting I-V and C-V plots were observed.

3.5 Results of RF-Sputtered AlN on Si – Effects of Nitrogen Flow rate during Deposition with Post Metal Anneal

3.5.1 Current-Voltage Characteristics

Fig. 3.5.1.1 shows the resulting I-V plots and Fig. 3.5.1.2 shows the corresponding J-E plots. The best leakage current results were obtained for a nitrogen flow rate of 30 sccm.

Hence, a comparison between the leakage currents of Al-AlN-Si MIS capacitor deposited with a nitrogen flow rate of 30sccm with and without PMA is shown in Fig 3.5.1.3. As it can be seen, the leakage current has decreased significantly following PMA and the breakdown voltage has also improved by 3V. This is because furnace annealing is reported to decrease lattice strain and microvoids, dislocations and other structural defects. This forms a layer with better stoichiometry and crystallinity. As a result, the breakdown voltage improves and the leakage current decreases. The results are summarised in Table 3.5.1.1.

Table 3.5.1.1: Results of Flow Rate optimization after PMA

Time of Deposition	N2 Flow Rate	t_{ox}	$J_{leakage}$ at $-2\,MV/cm$
20mins	10sccm	10nm	1.258×10^{-6}
20mins	20sccm	10nm	1.065×10^{-8}
20mins	30sccm	11nm	1.014×10^{-8}

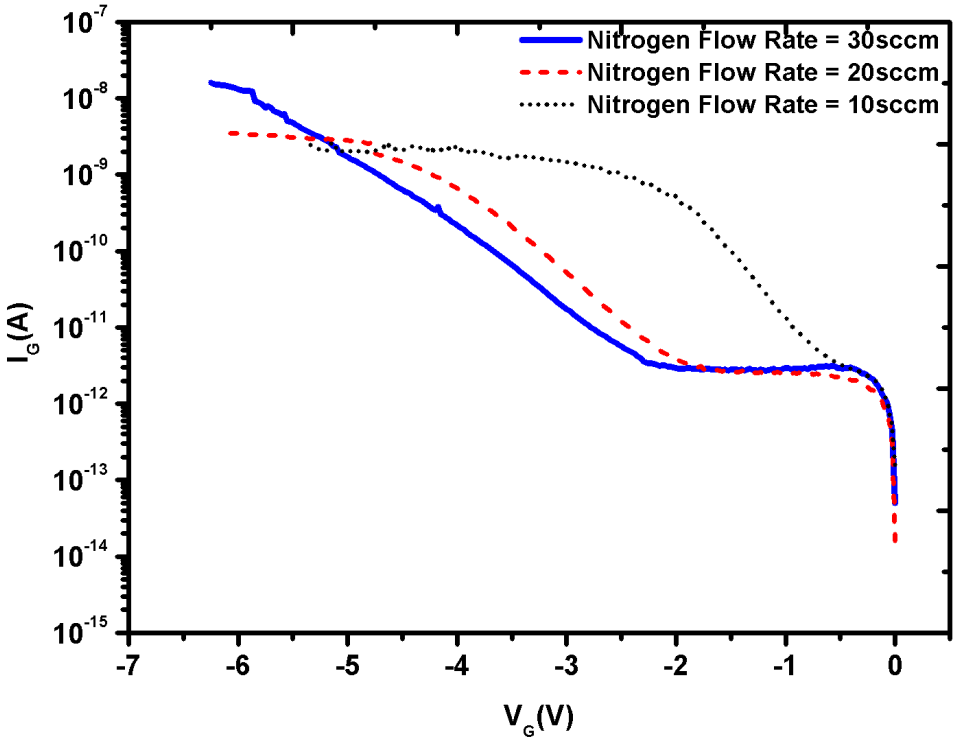

Fig 3.5.1.1: I-V characteristics of RF-sputtered MIS capacitors at different N_2 flow rates after PMA

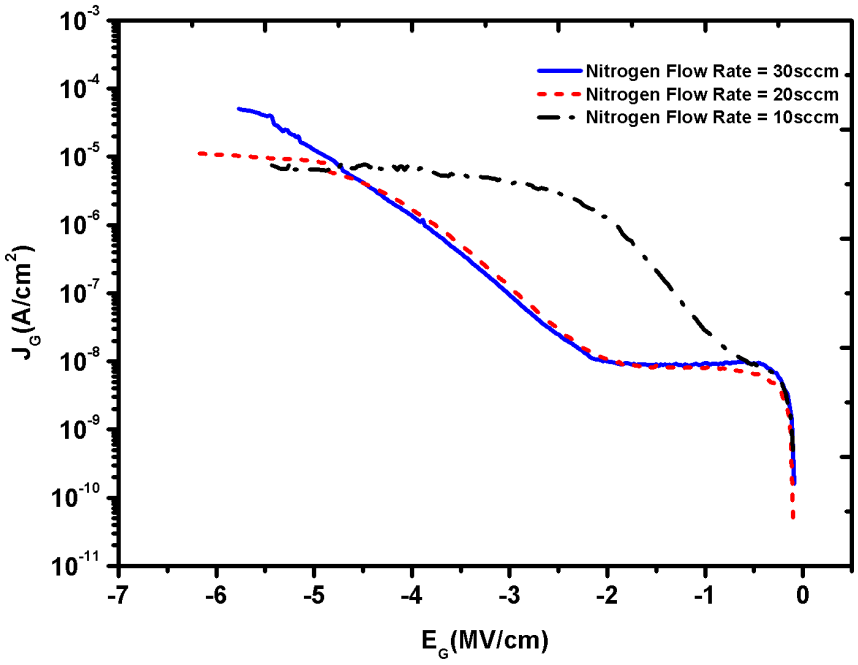

Fig 3.5.1.2: J-E characteristics of RF-sputtered MIS capacitors at different N_2 flow rates after PMA

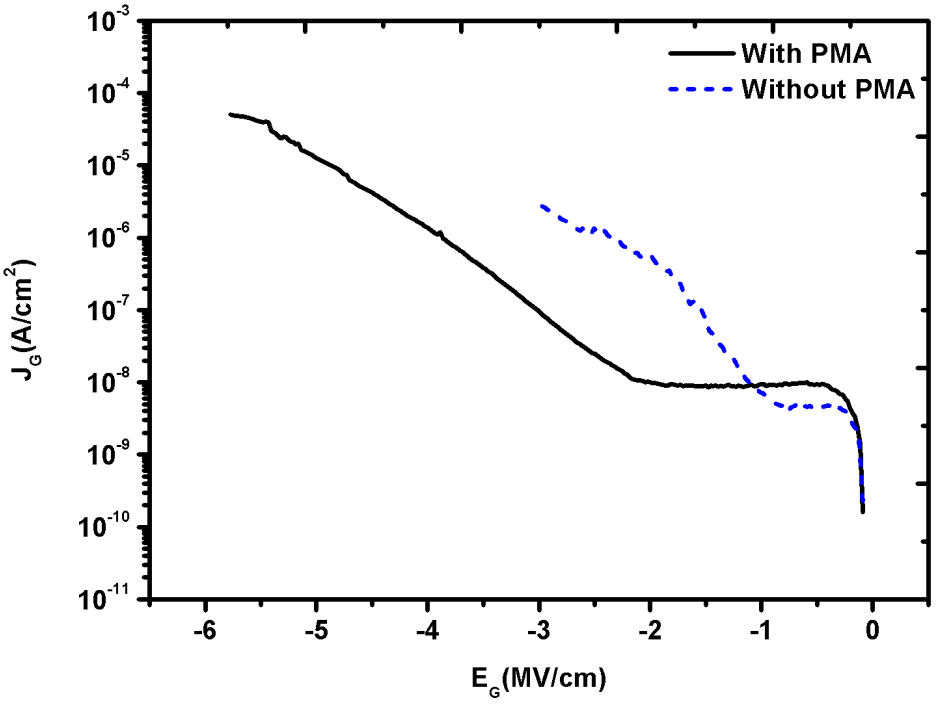

Fig 3.5.1.3: J-E characteristics comparison of RF-sputtered MIS capacitors with and without PMA

3.5.2 Capacitance-Voltage Characteristics

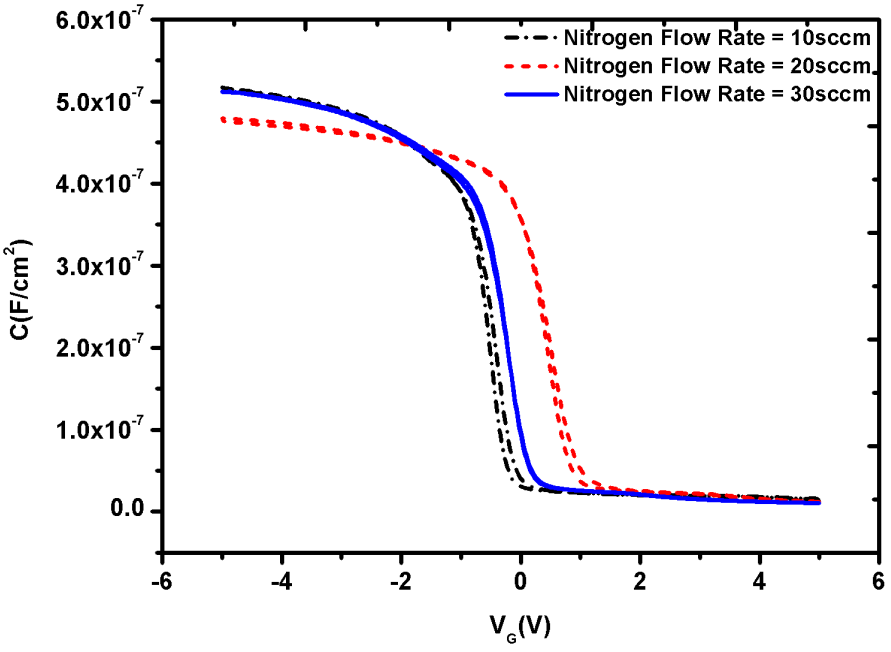

Fig 3.5.2.1: C-V characteristics of RF-sputtered MIS capacitors at different N_2 flow rates after PMA

Fig 3.5.2.1 shows the high frequency C-V measurements obtained after PMA. The capacitance is seen to reach saturation and a good accumulation capacitance is obtained. The MIS capacitors built with 30 sccm nitrogen show the least amount of hysteresis, indicating the least amount of interface traps. The flatband voltage shows a positive shift. This means there is a reduction in effective positive fixed charges in the interface. The dielectric constant extracted from the C-V curves is 7.2, which is close to reported value [16].

3.6 Experiment Details of RF-Sputtered AlN on Si – Effects of Post Deposition Anneal Time

From the previous section(3.5), it has been observed that maintaining a higher N_2/Ar flow rate ratio during the RF sputtering mechanism gives a better deposition in terms of morphology and crystallinity, which in turn the best leakage current characteristics and the capacitance characteristics with the least amount of hysteresis. Hence, the flow rate of N_2 was maintained at 30 sccm, with Ar flow rate being 20 sccm.

All the experiments were carried out on p-type Si substrate of 1-10Ω resistivity. The samples were cleaned and degreased in organic solvents followed by piranha cleaning and dilute Hydrofluoric acid (dil. HF) dip for few seconds. Then they were cleaned in nitric acid and again subjected to dil. HF dip. After each step, the samples were thoroughly rinsed in de-ionised water and blow-dried in N_2 to make sure the native oxide in Si substrate is removed completely.

Immediately after cleaning, the samples were loaded into the RF-sputtering system. The target was of AlN with *2 inch* diameter and of *99.5% purity*. The system chamber was evacuated using a turbo pump until a base pressure of less than $4.5 \times 10^{-7}\, mBar$ was reached. High purity argon was then introduced into the chamber following which the optimum deposition pressure of $1.0 - 1.5 \times 10^{-2} mBar$ was maintained. Nitrogen gas of high purity was then introduced into the chamber. The target was pre-sputtered for 10 minutes prior to deposition with a closed shutter to remove any oxides on the surface. The shutter was then opened and AlN was deposited on Si substrates. The details of sputtering parameters are summarized in Table 3.6.1

Table 3.6.1: RF Sputtering Parameters for PDA optimization

Substrate Temperature	Room Temperature
RF Power	100W

Argon Flow Rate	20sccm
Nitrogen Flow Rate	30sccm
Deposition Time	20mins
Deposition Pressure	$1.0 - 1.5 \times 10^{-2} mBar$

Following deposition, the samples were loaded for Post-Deposition Annealing (PDA) for different time periods. The furnace was ramped up to a temperature of $400℃$. The corresponding samples were loaded in to the furnace, and annealed for different time durations – 0mins, 10mins, 20mins and 30mins.

The samples were then loaded for Al metal deposition to form the gate metal. It was then patterned to form MOS capacitors of diameter$200\mu m$. Following this, the back-surface of the substrate was given buffered hydrofluoric acid (BHF) dip in order to remove the native back oxide and Al was deposited on the entire back surface to serve as Ohmic contact. Current-voltage (I-V) measurements and high frequency (1 MHz) capacitance-voltage (C-V) measurements were carried out in dark conditions at room temperature using Agilent's B1500A and using Agilent's B1500A and Cascade Microtech 1100 probe station. The resulting I-V and C-V plots were observed.

3.7 Results of RF-Sputtered AlN on Si – Effects of Post Deposition Anneal Time

3.7.1 Thickness

After RF-sputtered deposition, the thickness of deposited AlN layer was found to be 11nm by measuring with ellipsometer.

3.7.2 Current-Voltage Characteristics

The current versus voltage characteristics comparison of AlN deposited and annealed at $400℃$ for different time durations is shown in Fig 3.7.2.1. The corresponding current density versus electric field plot is shown in Fig 3.7.2.2. It can be seen that the leakage current reduces as the time of annealing increases. The reason can be that with annealing duration the Al-N bond density increases, and there is a possible increase in the nitrogen concentration of the film.

During the deposition of the nitride layer, there could be strain in the layer. There is a possibility of structural defects, voids being formed, inhomogeneity, grain boundaries, discontinuities etc., in case of vacuum deposited films. These defects can give rise to higher

leakage currents. For the removal of these defects, thermal energy provided by thermal annealing process is required [24].

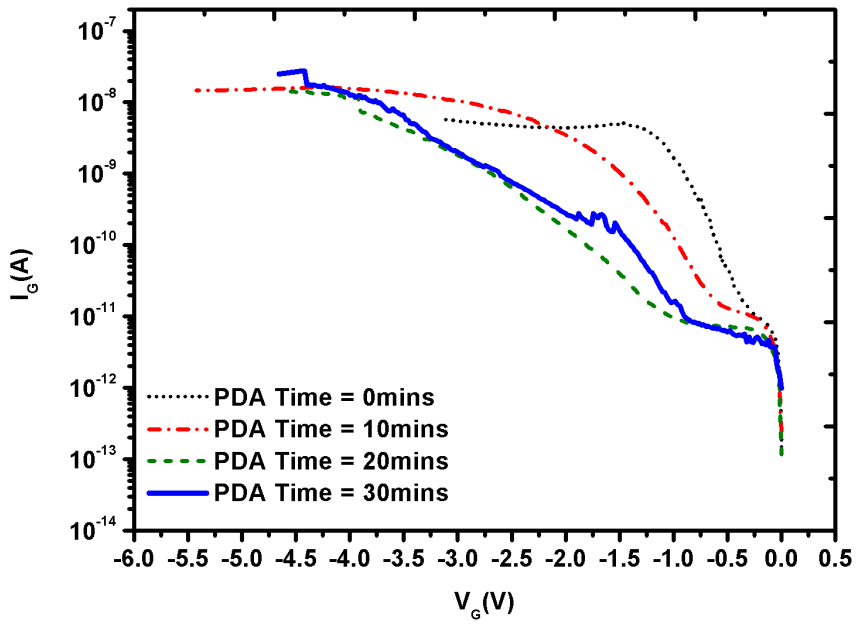

Fig 3.7.2.1: I-V characteristics of RF sputtered AlN MIS capacitors with different PDA Times

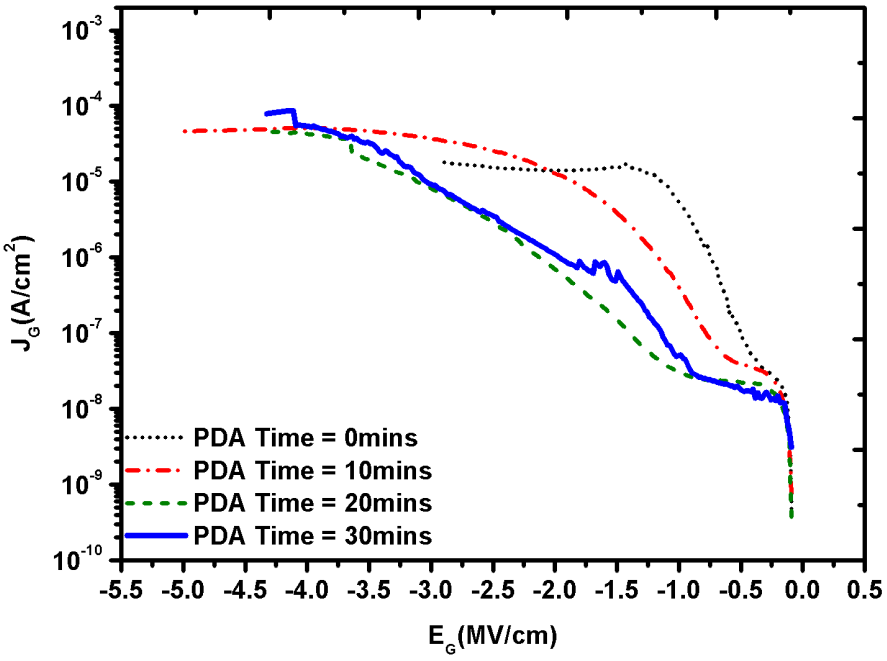

Fig 3.7.2.2: J-E characteristics of RF sputtered AlN MIS capacitors with different PDA Times

The conventional furnace annealing process in this case allows sufficient time for the atoms to get kinetic energy. On acquiring energy, they occupy equilibrium lattice positions which lead to the reduction in defects formed [21]. The leakage current reduces as a result.

The leakage current characteristics reduce with increase in annealing time. The characteristics obtained for 20mins 30mins of post-deposition annealing are comparable, showing saturation in the improvement provided by annealing at a low-annealing temperature of 400℃. Hence a PDA time of 20 mins or 30 mins observed to be the best parameters in case of 400℃ post deposition annealing. The results are summarised in Table 3.7.2.1.

Table 3.7.2.1: Results of Flow Rate optimization after PDA.

Time of Post Deposition Anneal	$J_{leakage}$ at $-2\,MV/cm$
0mins	1.413×10^{-5}
10mins	1.288×10^{-5}
20mins	7.058×10^{-7}
30mins	1.102×10^{-6}

3.7.3 Capacitance-Voltage Characteristics

The capacitance versus voltage (C-V) characteristics of the AlN RF-sputtered layers subjected to post deposition annealing for different time durations are shown in Fig 3.7.3.1. A small hysteresis can be observed in the C-V plot. The amount of hysteresis can be seen to increase with the duration of post-deposition annealing and is around 0.5V for a PDA time of 30mins. The positive shift of flat-band increases with increase in post deposition annealing time which shows the reduction of effective positive charges with PDA-time.

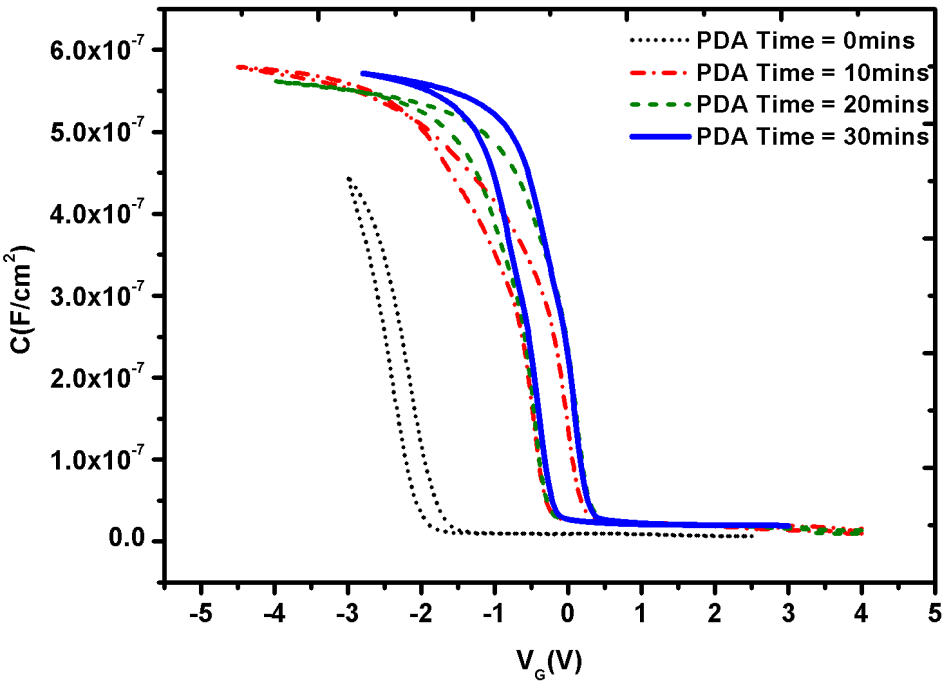

Fig 3.7.3.1: C-V characteristics of RF sputtered AlN MIS capacitors with different PDA Times

3.8 Experiment Details of RF-Sputtered AlN on Si with Post Deposition Anneal – Effects of Post Metalization Anneal

In the previous section, we have seen that subjecting the fabricated Al-AlN-MIS capacitors to post metalization anneal at 400℃ for 15mins improved the leakage current characteristics and the capacitance characteristics showed the accumulation saturation. To observe further improvement in the RF-sputtered AlN MIS capacitors with PDA, the devices were subjected to post-metalization anneal as well.

The temperature of the furnace was ramped up to 400℃ with the nitrogen flow rate maintained between 70and 80 litre/hr. The samples were loaded into the annealing furnace with a nitrogen flow rate of 120 litre/hr. They were then annealed in full nitrogen ambient at 400℃ for 15 mins. The samples were then taken out of the furnace and the temperature of the furnace was ramped down.

Current-voltage (I-V) measurements and high frequency (1 MHz) capacitance-voltage (C-V) measurements were carried out in dark conditions at room temperature using Agilent's

B1500A and Agilent's B1500A and Cascade Microtech 1100 probe station. The resulting I-V and C-V plots were observed.

3.9 Results of RF-Sputtered AlN on Si with Post Deposition Anneal – Effects of Post Metalization Anneal

3.9.1 Current-Voltage Characteristics

The current versus voltage characteristics comparison of AlN deposited and annealed at **400**℃ for different time durations is shown in Fig 3.9.1.1. The corresponding current density versus electric field plot is shown in Fig 3.9.1.2. It can be seen that the leakage current mechanism changes when both post deposition anneal and post metalization anneal is implemented. The reasons for this are not clear and need to be further investigated.

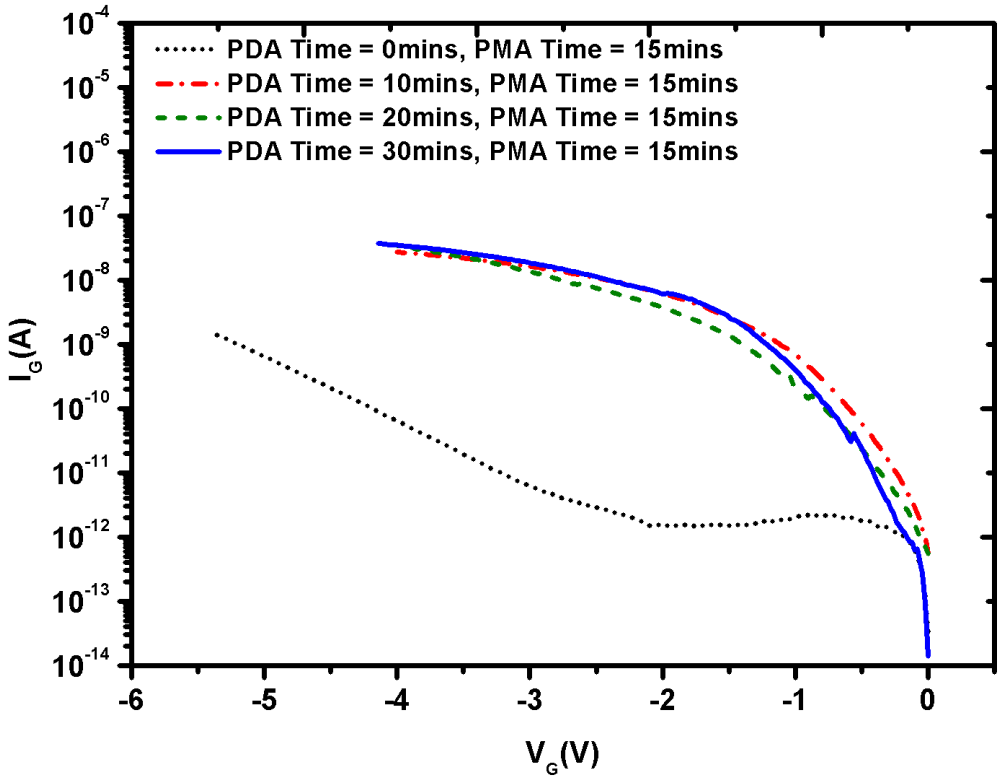

Fig 3.9.1.1: I-V characteristics of RF sputtered AlN MIS capacitors with different PDA Times and PMA of 15mins

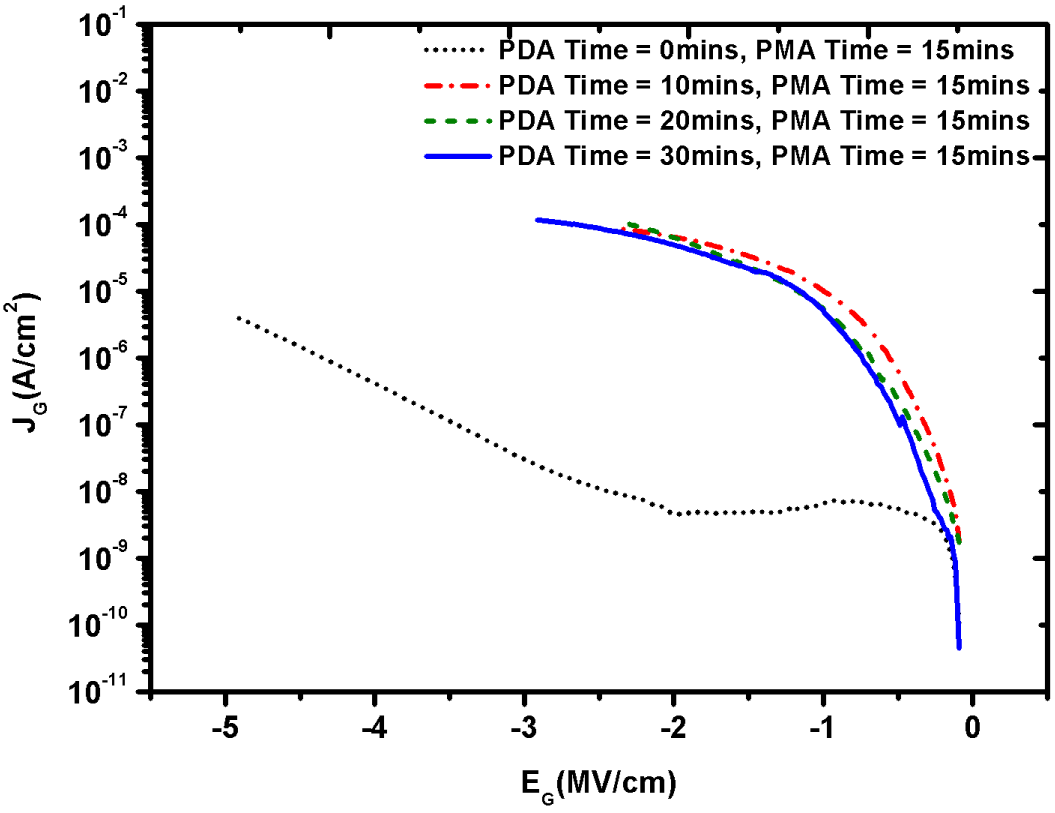

Fig 3.9.1.2: J-E characteristics of RF sputtered AlN MIS capacitors with different PDA Times and PMA of 15mins

3.9.2 Capacitance-Voltage Characteristics

The capacitance versus voltage (C-V) characteristics of the AlN RF-sputtered layers subjected to post deposition annealing for different time durations subjected to post metalization annealing are shown in Fig 3.9.2.1. It can be observed that after PMA, the hysteresis has become negligible. This indicates that the interface charges have been compensated for. The plots also show the best saturation of accumulation capacitance for PDA time = 30mins. The dielectric constant extracted from accumulation capacitance is 7.48. This is in accordance with reported values [16].

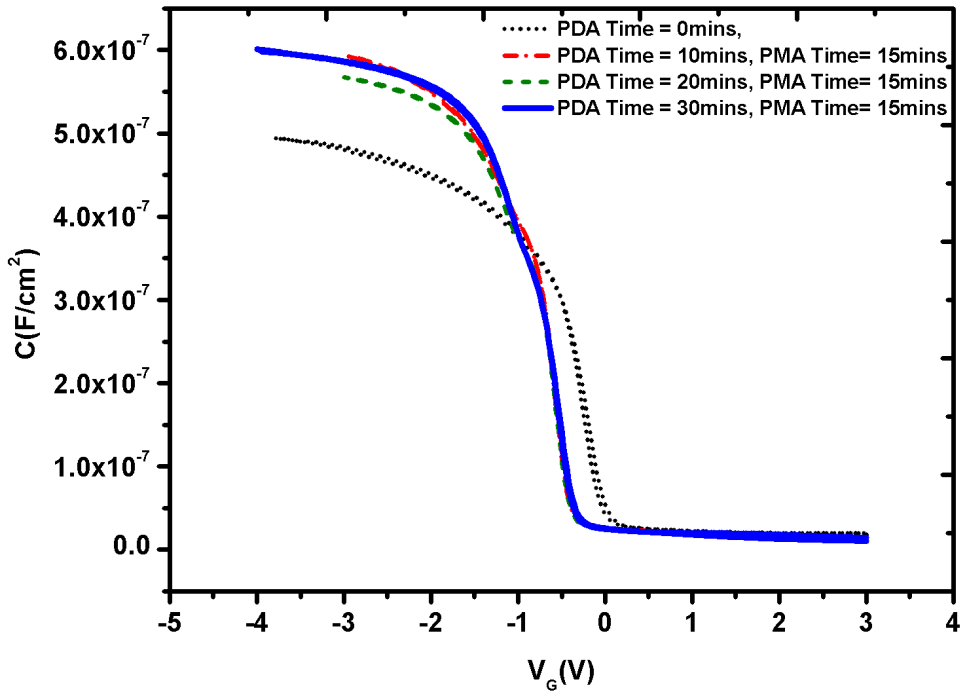

Fig 3.9.2.1: C-V characteristics of RF sputtered AlN MIS capacitors with different PDA Times and PMA Time=15mins

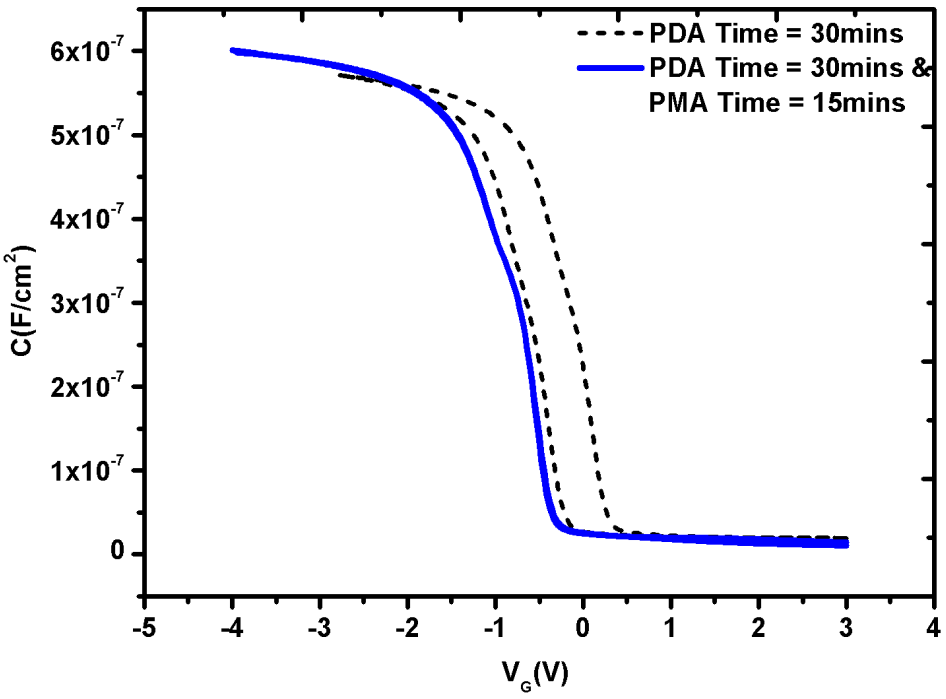

Fig 3.9.2.2: C-V characteristics comparison of RF sputtered AlN MIS capacitors for PDA and PDA with PMA

A comparison of the C-V characteristics of the RF-sputtered AlN MIS capacitors subjected to Post deposition annealing for 30mins at $400℃$ and post metalization annealing for 15mins at $400℃$ is shown in Fig 3.9.2.2. It can be seen that PMA decreases hysteresis and gives better C-V characteristics in the accumulation region.

3.10 Conclusions

The RF-sputtered deposition of AlN is carried out on Si to determine the optimum deposition conditions and subsequent annealing parameters to get a good MIS capacitor. The Nitrogen-Argon gas flow rate during RF-sputtering is varied and it is found that a high N_2/Ar ratio gives the best current and capacitance characteristics. Leakage currents density as low as $2.5 \times 10^{-7} A/cm^2$ at $-2\ MV/cm$ is obtained for a Nitrogen flow rate of 30sccm and Argon flow rate of 20sccm. The quality of AlN layer deposited improves with increase in N_2/Ar flow rate ratios. The devices were then subjected to post metalization annealing at $400℃$, which further improved the leakage current density to 1.014×10^{-8} at $-2\ MV/cm$. It also resulted in better capacitance characteristics in accumulation region. A positive flat band voltage shift was observed which indicates the effective reduction in positive insulator charges in the interface. A very low hysteresis window is observed.

The effect of low temperature ($400℃$) post deposition annealing time on the electrical characteristics of Al-AlN-Si MIS capacitors was studied. It is found that 20mins and 30mins give equivalent improvement in current characteristics. The current density observed was around7.058×10^{-7} at $-2\ MV/cm$. A hysteresis window of 0.5V is observed. Following this, the MIS capacitors are subjected to post-metal annealing which improve the capacitance characteristics in the accumulation region, and cancel the effect of interface charges.

Hence, the parameters are chosen to give optimum results for RF-sputtered deposition of AlN on Si for MIS capacitors are tabulated in Table 3.10.1

Table 3.10.1: Final Parameters obtained after optimization of parameters of RF-Sputtered ALN on SI MIS Capacitors

RF-Sputtered Deposition	
Substrate Temperature	Room Temperature
RF Power	100W
Argon Flow Rate	20sccm
Nitrogen Flow Rate	30sccm
Deposition Time	20mins
Deposition Pressure	$1.0 - 1.5 \times 10^{-2} mBar$
Post Deposition Anneal	
Time	30mins
Temperature	400℃
Post Metalization Anneal	
Time	15mins
Temperature	400℃

CHAPTER 4

RF Sputtered Deposition of AlN on SiC – Effects of Low Temperature Furnace Anneal

4.1 Introduction

It has been highlighted in the previous sections that SiC as a substrate semiconductor material has a lot of advantages over silicon. Because of its wide bandgap and high thermal conductivity, it is suitable for semiconductor power electronics.

AlN has a lattice match with SiC hence MIS Capacitors can be made with SiC as the semiconductor and AlN as the dielectric layer. In this chapter, we inspect the effectiveness of such a MIS capacitor in terms of its electrical characteristics.

4.2 Experiment Details of RF-Sputtered AlN on SiC - Effects of Post Deposition Anneal Time

All the experiments were carried out on n-type Si-face 4H-SiC bulk substrates. The samples were first cleaned in organic solvents to remove organic impurities. They were then cleaned in piranha, followed by buffered hydrofluoric acid (BHF) dip. Then they were subjected to cleaning in RCA1 and RCA2 with a BHF dip following each step. After each step, the samples were thoroughly rinsed in de-ionised water to make sure the native oxide in Si substrate is removed completely. Finally the samples are thoroughly blow dried with nitrogen.

Immediately after cleaning, the samples were loaded into the RF-sputtering chamber. The target was of AlN with *2 inch* diameter and of *99.5% purity*. The system chamber was evacuated using a turbo pump until a base pressure of less than $4.5 \times 10^{-7}\, mBar$ was reached. High purity argon was then introduced into the chamber following which the optimum deposition pressure of $1.0 - 1.5 \times 10^{-2} mBar$ was maintained. Nitrogen gas of high purity was then introduced into the chamber. The target was pre-sputtered for 10

minutes prior to deposition with a closed shutter to remove any oxides on the surface. The shutter was then opened and AlN was deposited on SiC substrates.

The optimum conditions for deposition were obtained from the optimization experiments done on Si substrate, which has been elaborated in the previous chapter. The details of sputtering parameters are summarized in Table 4.2.1.

Table 4.2.1: Parameters of RF-Sputtering For Deposition of AlN on SiC

Substrate Temperature	Room Temperature
RF Power	100W
Argon Flow Rate	20sccm
Nitrogen Flow Rate	30sccm
Deposition Time	20mins
Deposition Pressure	$1.0 - 1.5 \times 10^{-2} mBar$

For Si, a post deposition anneal time of 30mins in a temperature of $400℃$ gave the best electrical characteristics for AlN dielectric layer, as observed in the previous section. To study the effect of post deposition annealing time on Al-AlN-SiC MIS capacitor, two different sets of experiments are carried out – one without PDA (i.e. PDA time = 0mins), the other one with a PDA time of 30 mins.

Following deposition, the samples were loaded for Post-Deposition Annealing (PDA) for different time periods. The furnace was ramped up to a temperature of $400℃$. The corresponding samples were loaded in to the furnace, and annealed for different time durations – 0mins and 30mins.

The samples were then loaded for Al metal deposition to form the gate metal. It was then patterned to form MOS capacitors of different diameters. Following this, the back-surface of the substrate was given buffered hydrofluoric acid (BHF) dip in order to remove the native back oxide and Al was deposited on the entire back surface to serve as Ohmic contact. Current-voltage (I-V) measurements and high frequency (1 MHz) capacitance-voltage (C-V) measurements were carried out in dark conditions at room temperature using Agilent's B1500A and Agilent's B1500A and Cascade Microtech 1100 probe station. The resulting I-V and C-V plots were observed.

4.3 Results of RF-Sputtered AlN on SiC- Effects of Post Deposition Anneal Time

4.3.1 Thickness

The MIS capacitors thus prepared were characterised for observations. After RF-sputtered deposition, the thickness of deposited AlN layer was found to be 7.15nm by measuring with ellipsometer. The variation in thickness obtained inspite of using the same deposition parameters was because there was a change in the distance between the target and the position of the samples, which resulted in a slower rate of deposition.

4.3.2 Current-Voltage Characteristics

The current density versus voltage plots of the RF-sputtered AlN MIS capacitors subjected to Post deposition annealing for 0mins and 30mins at 400℃ are given in Fig 4.3.2.1, and the Current-density versus electric field characteristics are given in Fig 4..3.2.2.

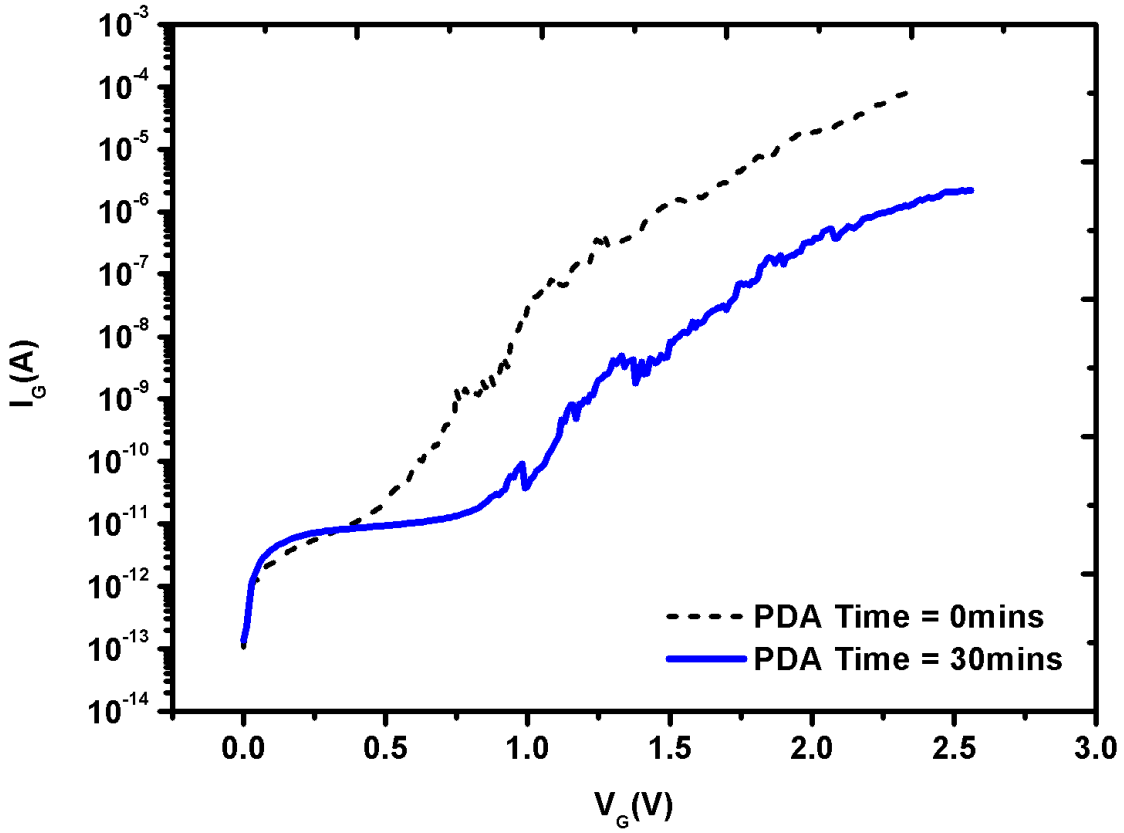

Fig 4.3.2.1: I-V Characteristics of RF-Sputtered AlN on SiC MIS Capacitors with different PDA Times

The breakdown voltages of the MIS capacitors were measured, and all the I-V characteristics were obtained till just until the breakdown voltage. As it can be seen, the post deposition annealing for 30mins improves the leakage current characteristics.

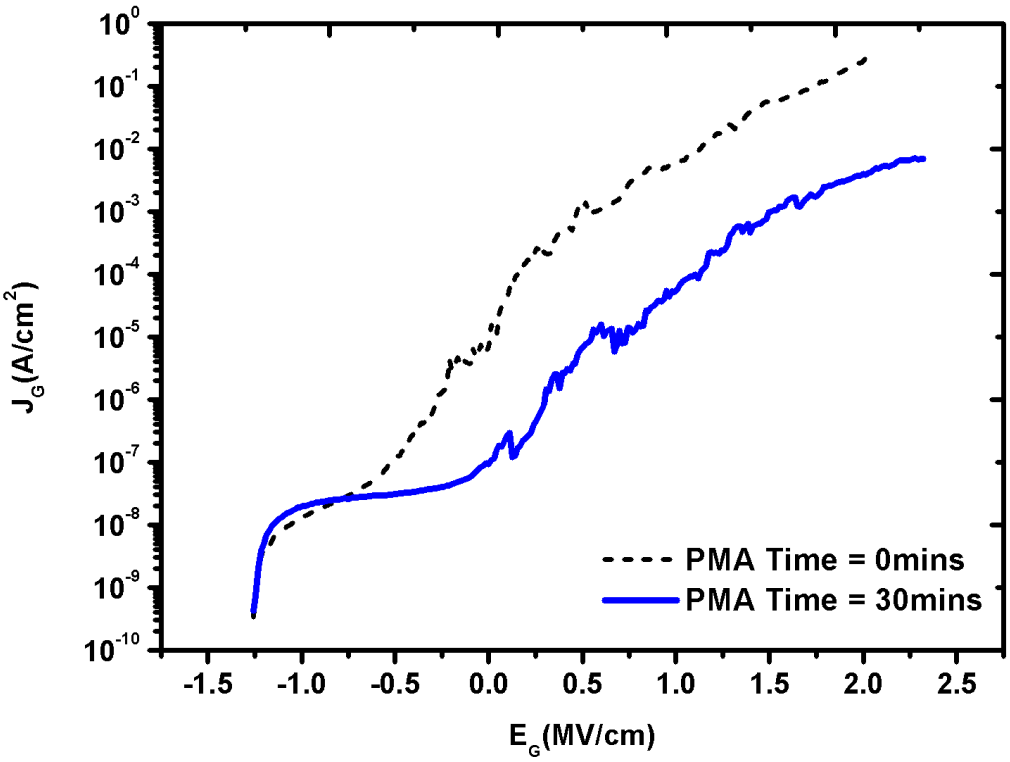

Fig 4.3.2.2: J-E Characteristics of RF-Sputtered AlN on SiC MIS Capacitors with different PDA Times

The breakdown field showed and improvement of 0.5 MV/cm and the leakage current density reduced from $5.64 \times 10^{-3}\, A/cm^2$ (PDA Time = 0mins) to $5.63 \times 10^{-5}\, A/cm^2$ (PDA Time = 30mins) at 1 MV/cm. The furnace annealing improves the smoothness of the AlN layer [23]. It also passivates defects and dislocations and reduces the concentration of traps. The results are summarised in Table 4.3.2.1

Table 4.3.2.1: Results of RF-sputtered AlN on SiC Capacitors after PDA in different time durations.

Time of Post Deposition Anneal	$J_{leakage}$ at 1 MV/cm (A/cm^2)
0mins	5.64×10^{-3}
30mins	5.63×10^{-5}

4.3.3 Capacitance-Voltage Characteristics

Fig 4.3.3.1 and Fig 4.3.3.2 shows the plots obtained for the capacitance-voltage characteristics. As it can be seen, correct C-V plots were not obtained because of a low-breakdown field. The capacitors could not be biased to a more positive voltage because of early breakdown. This indicates that the flatband voltage was a large positive value. This might have resulted from a large concentration of negative fixed insulator charges. Hence to obtain a correct C-V plot, an improvement in the breakdown field is required, so as to be able to bias the MIS capacitors to higher positive voltages.

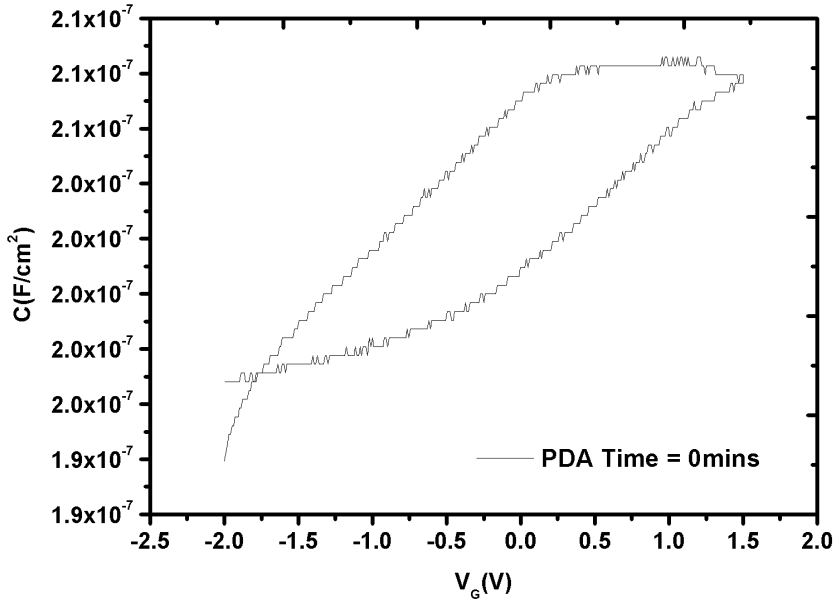

Fig 4.3.3.1: C-V Characteristics of RF-Sputtered AlN on SiC MIS Capacitors with PDA Time = 0mins

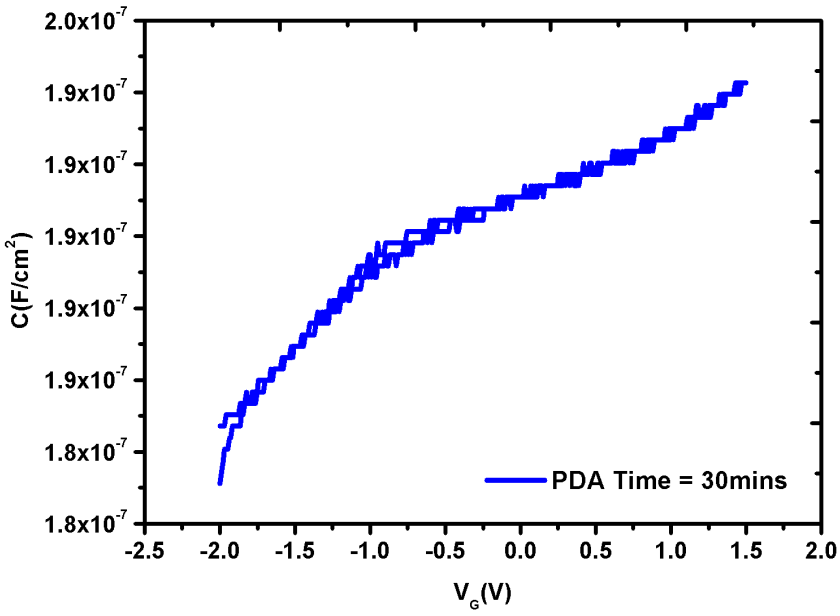

Fig 4.3.3.2: C-V Characteristics of RF-Sputtered AlN on SiC MIS Capacitors with PDA Time = 30mins

The parameters like dielectric constant, interface charge concentration and fixed charge concentration could not be obtained by high-frequency C-V measurements because the MIS capacitors did not reach accumulation region.

4.4 Experimental Details of RF-Sputtered AlN on SiC- Effects of Post Metalization Anneal

It has been seen in the previous chapter that the optimised values for post metalization anneal in Al-AlN-Si MIS capacitors was for 15mins at 400℃. Hence, the same parameters are adopted in the case of MIS capacitors with SiC as the substrate.

To study the effect of post-metalization anneal, two sets of experiments were done. One set of devices were subjected to only PMA, without PDA. Another set of devices were first subjected to PDA at 400℃ for 30mins, then PMA at 400℃ for 15mins.

The temperature of the furnace was ramped up to 400℃ with the nitrogen flow rate maintained between 70 and 80 litre/hr. The samples were loaded into the annealing furnace with a nitrogen flow rate of 120 litre/hr. They were then annealed in full nitrogen ambient at 400℃ for 15 mins. The samples were then taken out of the furnace and the temperature of the furnace was ramped down.

Current-voltage (I-V) measurements and high frequency (1 MHz) capacitance-voltage (C-V) measurements were carried out in dark conditions at room temperature using Agilent's B1500A and Agilent's B1500A and Cascade Microtech 1100 probe station. The resulting I-V and C-V plots were observed.

4.5 Results of RF-Sputtered AlN on SiC- Effects of Post Metalization Anneal

4.5.1 Current-Voltage Characteristics

The current density versus voltage characteristics of the RF-sputtered AlN MIS capacitors subjected to Post deposition annealing for 0mins and post metal annealing for 15mins at 400℃ are shown in Fig 4.5.1.1. MIS capacitors of different diameters were realised and characterised to obtain the resultant plots.

From the J-E plots shown in fig 4.5.1.2, we can infer that there is a large amount of surface leakage current, which increases with increasing area. For the devices with the smallest area ($4.126 \times 10^{-5} cm^2$) a greater breakdown field was obtained (3.88 MV/cm) because of lower surface leakage current.

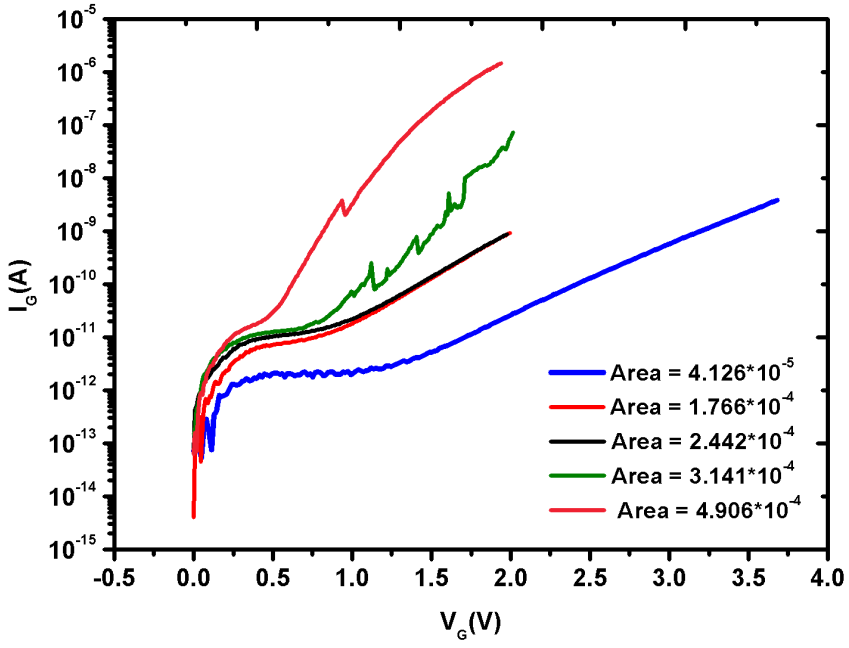

Fig 4.5.1.1: I-V Characteristics of RF-Sputtered AlN on SiC MIS Capacitors of different areas with PDA Time = 0mins, PMA Time = 15mins

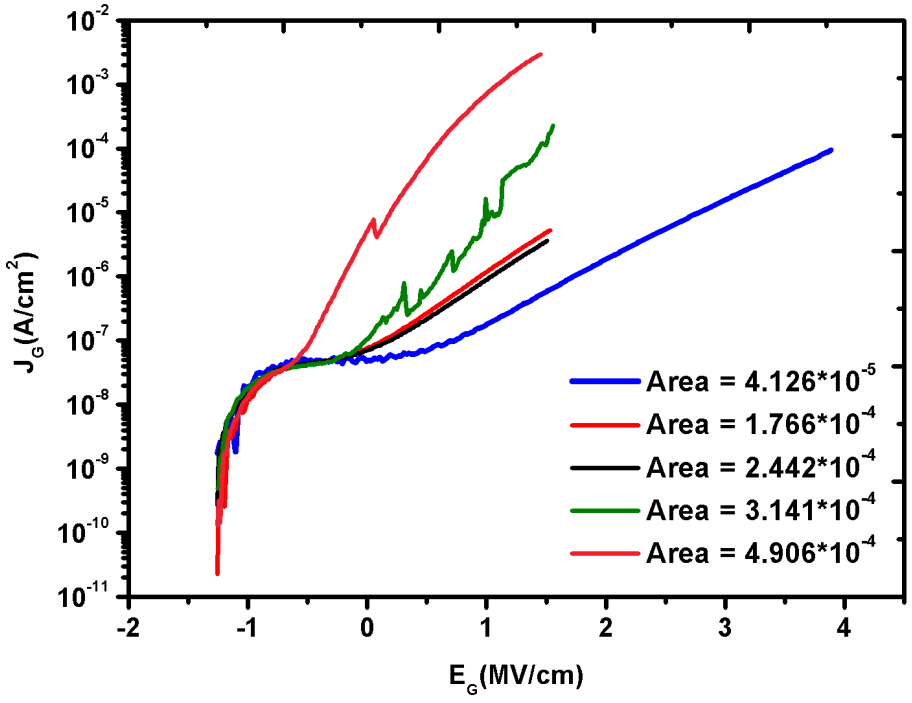

Fig 4.5.1.2: J-E Characteristics of RF-Sputtered AlN on SiC MIS Capacitors of different areas with PDA Time = 0mins, PMA Time = 15mins

Similarly, in Fig 4.5.1.3 the current density versus voltage characteristics of the RF-sputtered AlN MIS capacitors subjected to Post deposition annealing for 30mins and post metal annealing for 15mins at 400℃ are shown and Fig 4.5.1.4 represent the current density versus electrical field (J-E) characteristics of the same. We can observe that the breakdown field of the MIS capacitors has improved. The current mechanisms that come into play in this case seem to be varying, although further analysis needs to be done to explain the occurring phenomena. A comparison of the current densities for the smallest area ($4.126 \times 10^{-5} cm^2$) MIS capacitors has been shown in Fig 4.5.1.5. It can be seen that although the current degrades slightly in case of PDA and PMA compared to the only PMA processed devices, the former has improved breakdown voltage ($4.68\ MV/cm$) compared to the later ($3.88\ MV/cm$).

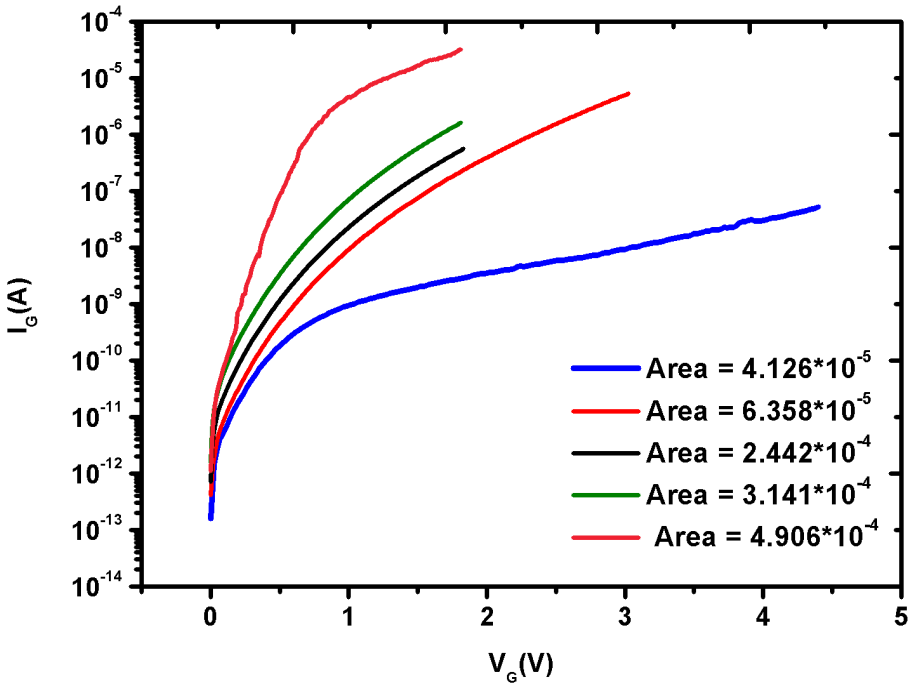

Fig 4.5.1.3: I-V Characteristics of RF-Sputtered AlN on SiC MIS Capacitors of different areas with PDA Time = 30mins, PMA Time = 15mins

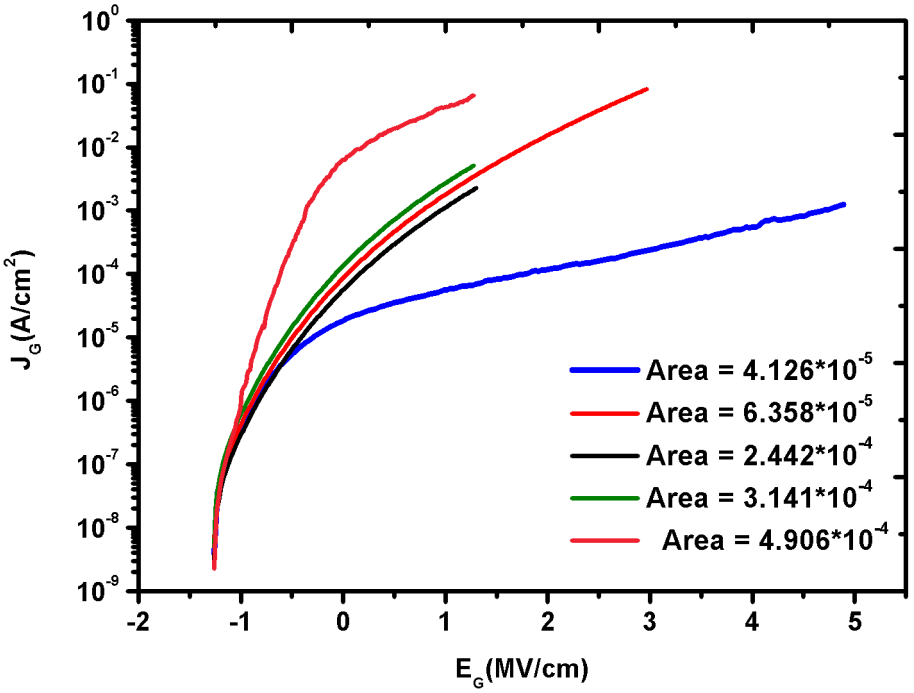

Fig 4.5.1.4: J-E Characteristics of RF-Sputtered AlN on SiC MIS Capacitors of different areas with PDA Time = 30mins, PMA Time = 15mins

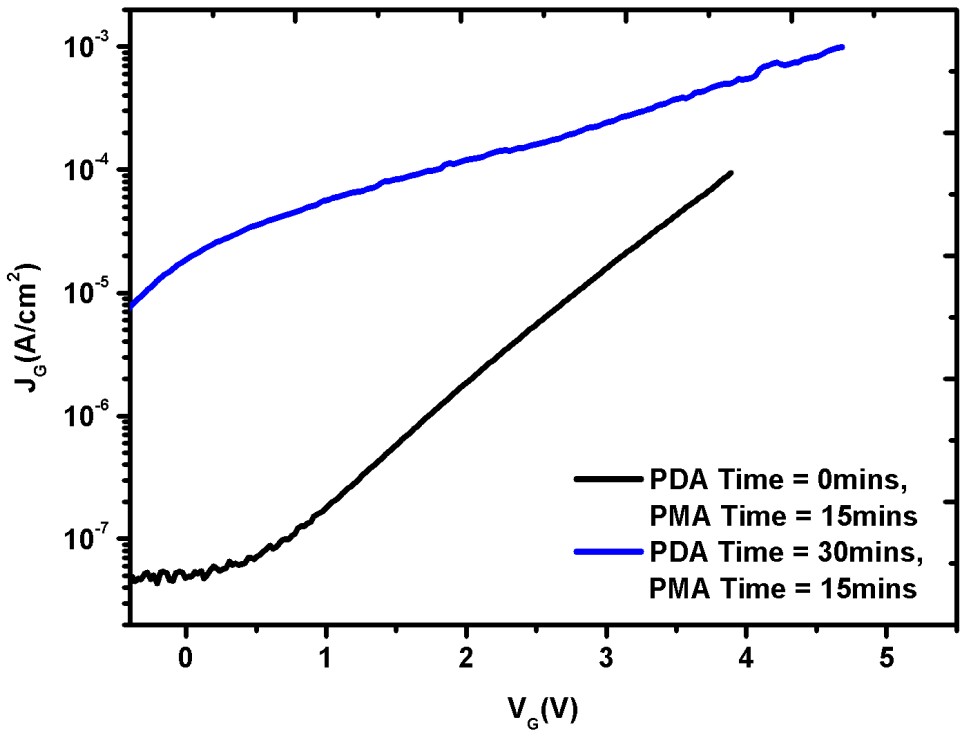

Fig 4.5.1.5: J-E Characteristics comparison of RF-Sputtered AlN on SiC MIS Capacitors with different PDATime and with PMA Time = 15mins

4.5.2 Capacitance-Voltage Characteristics

Fig 4.5.2.1 shows the C-V characteristics obtained from RF-sputtered AlN MIS capacitors subjected to Post deposition annealing for 0mins and post metal annealing for 15mins at 400℃. Again, we can see that the capacitance plots obtained were not correct, since they could not be characterised to higher voltages.

The C-V characteristics obtained from RF-sputtered AlN MIS capacitors subjected to Post deposition annealing for 30mins and post metal annealing for 15mins at 400℃ are shown in Fig 4.5.2.2. The capacitance reached accumulation region and is seen to start saturating. Very low hysteresis is observed in the C-V plots which show the reduction in the interface traps.

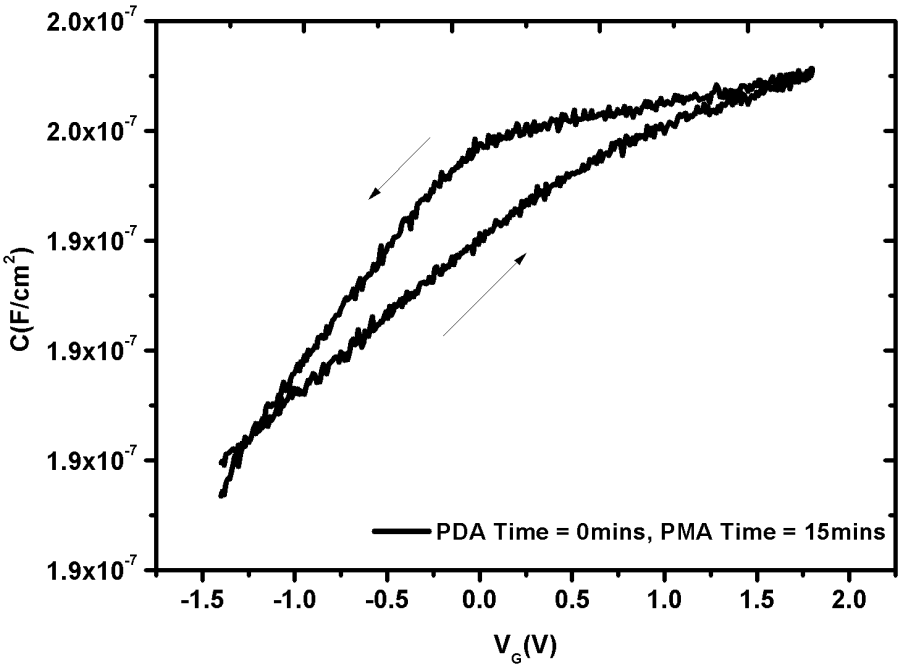

Fig 4.5.2.1: C-V Characteristics of RF-Sputtered AlN on SiC MIS Capacitors with PDA Time = 0mins, PMA Time = 15mins

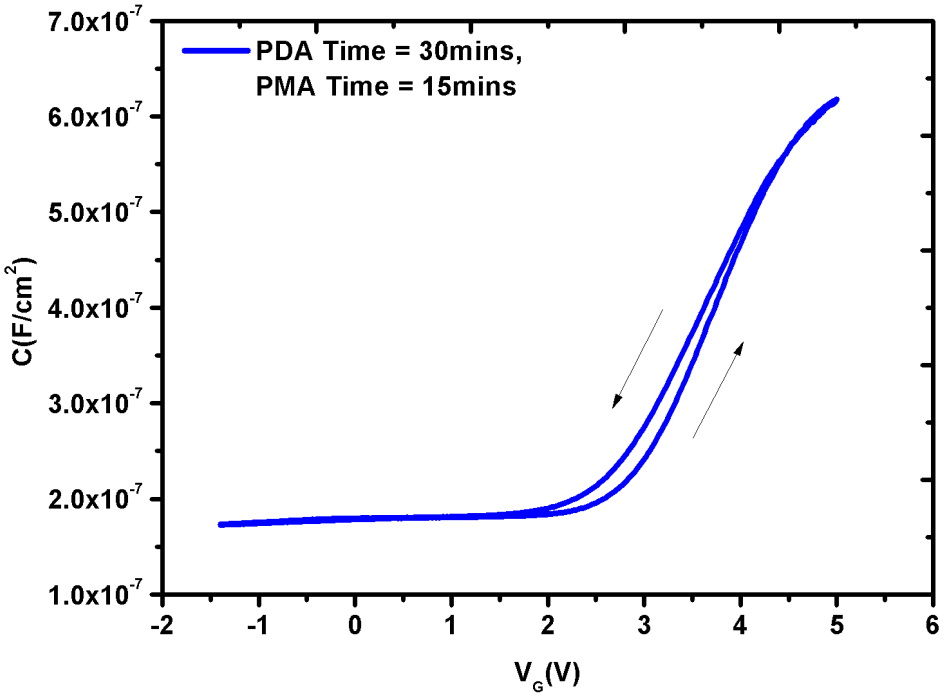

Fig 4.5.2.2: C-V Characteristics of RF-Sputtered AlN on SiC MIS Capacitors with PDA Time = 30mins, PMA Time = 15mins

The high frequency C-V measurements were used to extract the value of the dielectric constant of AlN by using the thickness of AlN layer measured with ellipsometer post deposition. The dielectric constant was obtained to be 4.9 for a layer of thickness of 7.15nm. This is in accordance with values reported in literature, where it is observed that the dielectric constant calculated from the maximum capacitance was between 2-6 for layers below 10nm [16]. Using the calculated dielectric constant, the thickness of the dielectric layer is extracted, and the value (7.02nm) is in accordance with the ellipsometer-measured value (7.15nm).

From the high frequency C-V curve, the values of interface state density, D_{it}, are obtained using Terman's method. Fig 4.5.2.3 shows the D_{it} versus $E_C - E_T$ plot. The value of D_{it} is calculated to be 8.067×10^{13} at 0.5eV below the conduction band E_C.

The flat-band voltage is calculated to be 4.492V, which is large in the positive direction. The fixed insulator charge (Q_f) concentration is calculated to be $-1.397 \times 10^{13} cm^{-2}$. This large concentration of negative fixed insulator charge explains the high positive flat-band voltage. Thy hysteresis observed is very low, which might be due to the compensation of interface traps in the insulator.

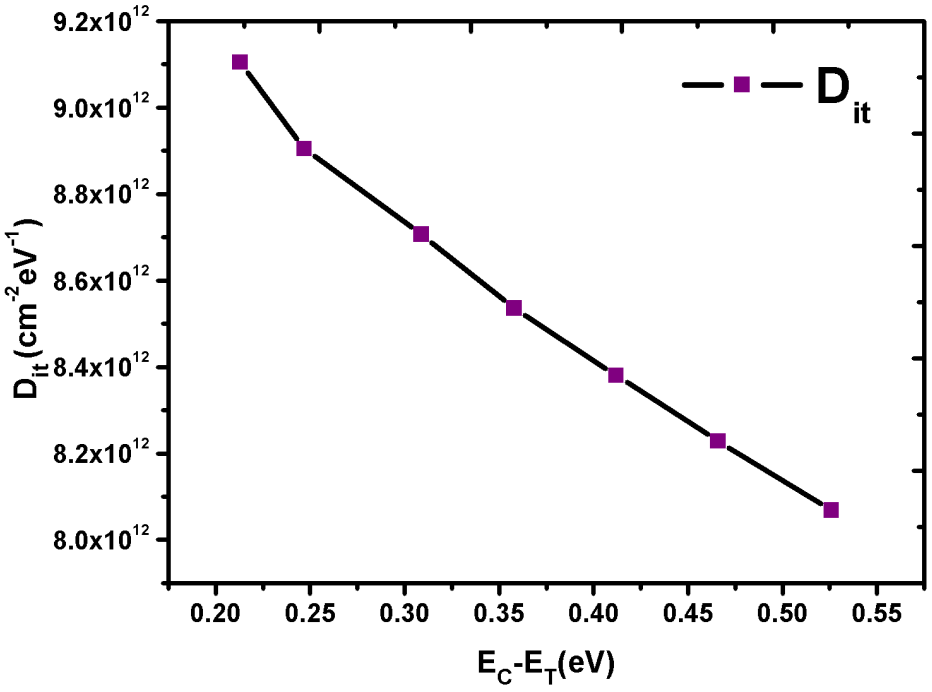

Fig 4.5.2.3: Interface Density as measured by Terman's Method of RF-Sputtered AlN on SiC MIS Capacitors with PDA Time = 30mins, PMA Time = 15mins

4.6 Conclusions

The RF-sputtered Al-AlN-SiC MIS capacitors were studied with respect to the effects of post deposition anneal and post metalization anneal time at a temperature of 400℃. The devices processed with post deposition anneal for 30mins showed better leakage current densities compared to the device without post deposition anneal which is summarised in Table 4.1. But the breakdown field achieved is low, because of which the MIS capacitors could not be biased to higher voltages to reach accumulation region. This also indicates a positive flat-band voltage shift.

The effect of post metalization anneal time is studied next. It has been found that the devices subjected to only PMA for 15mins at 400℃ showed better leakage current values compared to those subjected to both PDA (30mins, 400℃) and PMA (15mins, 400℃). The slight degradation in current-voltage characteristics in the latter's case could not be explained. But the latter showed improvement in the breakdown field than the former. Because of the improvement in breakdown field, the MIS capacitors could be biased to higher positive voltages and the capacitance-voltage curves reached accumulation region. The large positive shift in flatband voltage is attributed to the large concentration of negative fixed insulator charge concentration, which is further confirmed by the calculated values of Q_f. The interface state density, D_{it}, obtained using Terman's method is 8.067×10^{13} at 0.5eV below the conduction band E_C.

Hence to obtain a good Al-AlN-MIS capacitor, both post deposition anneal and post metalization anneal is needed.

CHAPTER 5

RF Sputtered Deposition of AlN on SiC – Effects of Rapid Thermal Anneal

5.1 Introduction

Al-AlN-SiC MIS capacitors have been fabricated by using RF-sputtered deposition process and furnace based post deposition annealing and post metalization annealing have been applied. In the previous chapter, we have seen that the MIS capacitors made using the optimised parameters of fabrication show low leakage current levels and capacitance-voltage characteristics. However, it is desired to obtain further low levels of leakage current.

Rapid thermal annealing has been used to improve the film quality of AlN dielectric layer as a post deposition process. It has been earlier reported that films having a clear c-axis orientation show significant improvement in quality when subjected to rapid thermal annealing. RF-sputtered AlN films are typically found to have c-axis orientations. Although the lattice mismatch between AlN and SiC is supposed to be less than 1%, there can be higher mismatch because of deposition conditions. This can produce a high density of dislocations which can act as non-radiative recombination centres [8]. Rapid thermal annealing is known to improve the crystallinity of the ALN layer and reduce dislocations as well.

The motivation was to explore different RTA conditions with respect to time and temperature in order to obtain low leakage currents in AlN thin film dielectric. Hence, RTA is used as a post deposition annealing process.

5.2 Experimental Details of RF-Sputtered AlN on SiC- Effects of Rapid Thermal Anneal

All the experiments were carried out on n-type Si-face 4H-SiC bulk substrates. The samples were first cleaned in organic solvents to remove organic impurities. They were then cleaned in piranha, followed by buffered hydrofluoric acid (BHF) dip. Then they were subjected to cleaning in RCA1 and RCA2 with a BHF dip following each step. After each step, the

samples were thoroughly rinsed in de-ionised water to make sure the native oxide in Si substrate is removed completely. Finally the samples are thoroughly blow dried with nitrogen.

Immediately after cleaning, the samples were loaded into the RF-sputtering chamber. The target was of AlN with *2 inch* diameter and of *99.5% purity*. The system chamber was evacuated using a turbo pump until a base pressure of less than $4.5 \times 10^{-7}\, mBar$ was reached. High purity argon was then introduced into the chamber following which the optimum deposition pressure of $1.0 - 1.5 \times 10^{-2} mBar$ was maintained. Nitrogen gas of high purity was then introduced into the chamber. The target was pre-sputtered for 10 minutes prior to deposition with a closed shutter to remove any oxides on the surface. The shutter was then opened and AlN was deposited on SiC substrates.

The optimum conditions for deposition were obtained from the optimization experiments done on Si substrate, which has been elaborated in the previous chapter. The details of sputtering parameters are the same as in Table 4.2.1.

Following deposition, the samples were loaded in into Annealsys Rapid Thermal Processing cold wall chamber furnace. The temperature was ramped up after purging the system with high purity nitrogen gas. The time and temperature of the RTA process was set according to requirements. Following RTP, a slightly larger cool down time was allowed to avoid cracks in the substrate.

The samples were then loaded for Al metal deposition to form the gate metal. It was then patterned to form MOS capacitors of different diameters. Following this, the back-surface of the substrate was given buffered hydrofluoric acid (BHF) dip in order to remove the native back oxide and Al was deposited on the entire back surface to serve as Ohmic contact. Current-voltage (I-V) measurements and high frequency (1 MHz) capacitance-voltage (C-V) measurements were carried out in dark conditions at room temperature using Agilent's B1500A and Agilent's B1500A and Cascade Microtech 1100 probe station. The resulting I-V and C-V plots were observed.

5.3 Results of RF-Sputtered AlN on SiC- Effects of Rapid Thermal Anneal

5.3.1 Rapid Thermal Annealing at 900℃ for 10 seconds

The devices characterised in this section were exposed to RTA for 10 second at a temperature of 900℃. The initial set of RTA parameters was chosen according to literature reports [9]. The thickness of the deposited AlN layer was found to be 7nm by measuring with ellipsometer.

5.3.1.1 Current-Voltage Characteristics

The current density versus voltage plots of the RF-sputtered AlN MIS capacitors subjected to Post deposition rapid thermal annealing for 10 seconds at 900℃ are given in Fig 5.3.1.1.1, and the Current-density versus electric field characteristics are given in Fig 5.3.1.1.2.

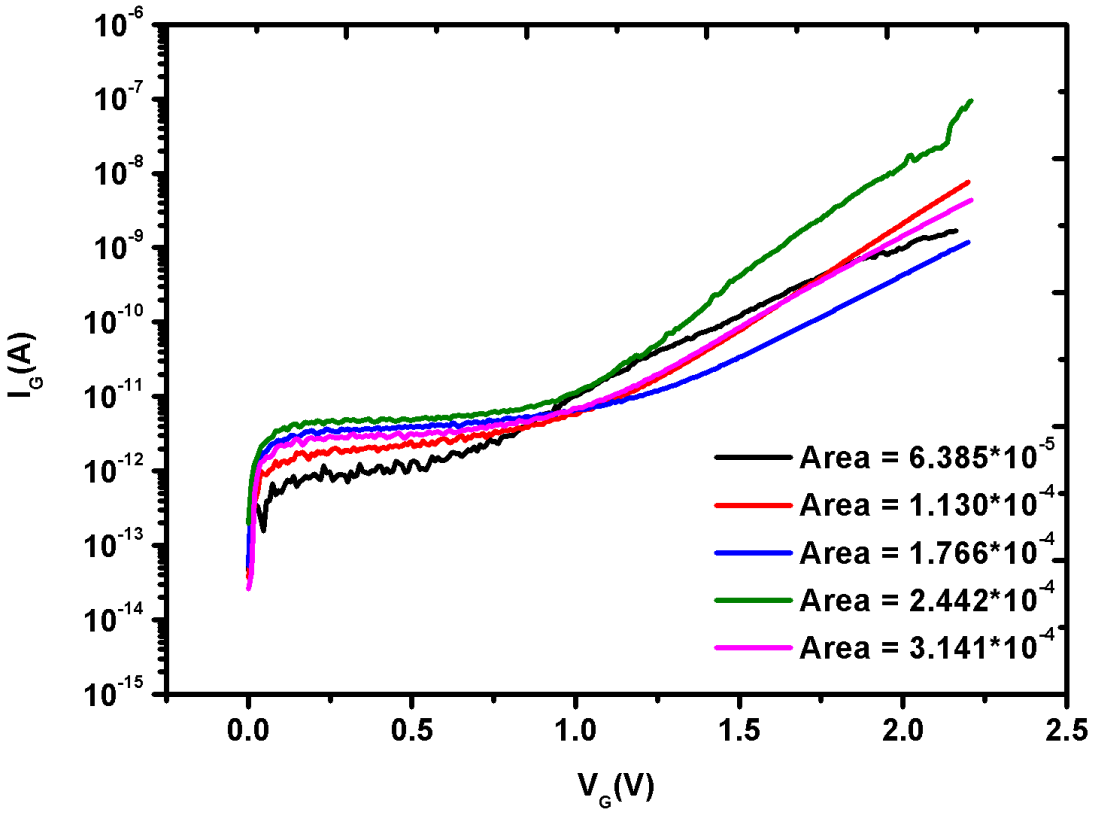

Fig 5.3.1.1.1: I-V Characteristics of RF-Sputtered AlN on SiC MIS Capacitors of different areas with RTA temperature= 900℃ and Time = 10 sec

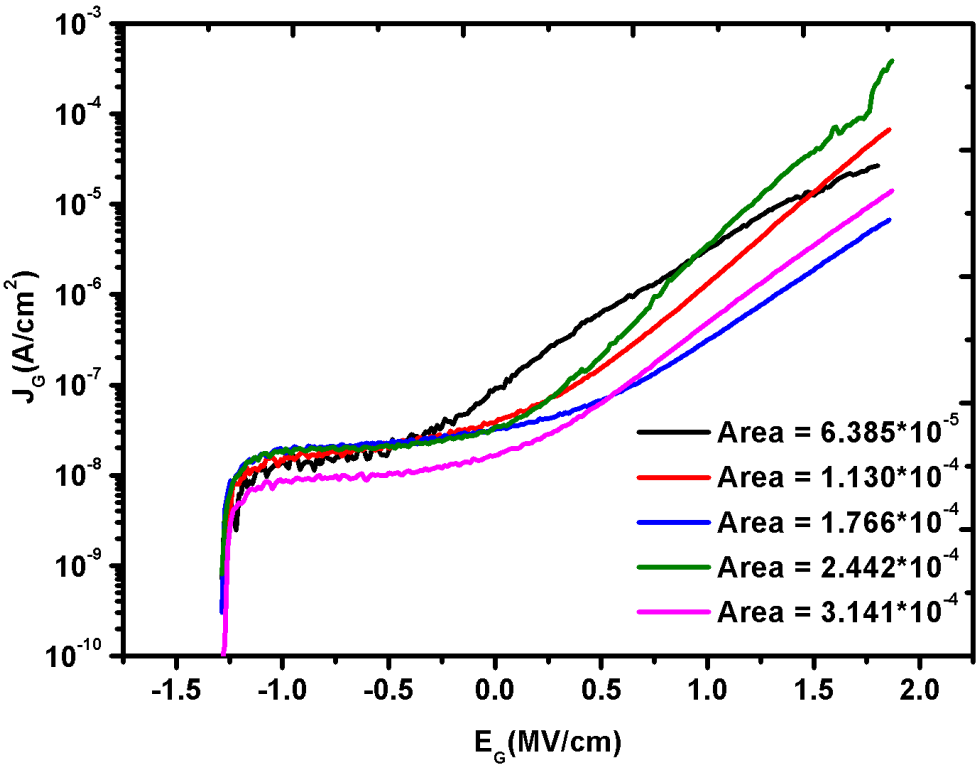

Fig 5.3.1.1.2: J-E Characteristics of RF-Sputtered AlN on SiC MIS Capacitors of different areas with RTA temperature= 900℃ and Time = 10 sec

It can be observed that very low leakage current densities are obtained with RTA. The variations in the current densities of MIS capacitors of different areas are not because of surface leakage but because of variations within the samples. Hence, the dependence of surface leakage current with area of capacitors is reduced significantly with RTA as compared to conventional furnace annealing results reported in a previous section.

RTA is reported to increase the Al-N bond density due to the diffusion of nitrogen into the film. The relationship of electrical properties and annealing depends a lot on grain boundaries and dislocations. The defects lead to the formation of traps in the insulator layer which affect the leakage current and capacitance characteristics.

The leakage current densities obtained for post deposition RTA is $4.861 \times 10^{-7} A/cm^2$ compared to $5.63 \times 10^{-5} A/cm^2$ for conventional furnace annealed current densities. Hence, about two orders smaller current densities were obtained with RTA compared to conventional furnace post deposition anneal.

5.3.1.2 Capacitance-Voltage Characteristics

Fig 5.3.1.2.1 shows the C-V characteristics obtained from RF-sputtered AlN MIS capacitors subjected to post deposition RTA for 10seconds at 900℃. Complete capacitance-voltage curves could not be obtained because of a high positive in flatband voltage. Only a section of the curves in the inversion region was obtained. Since the C-V curves did not reach accumulation region, further analysis of dielectric constant and charge concentration could not be done.

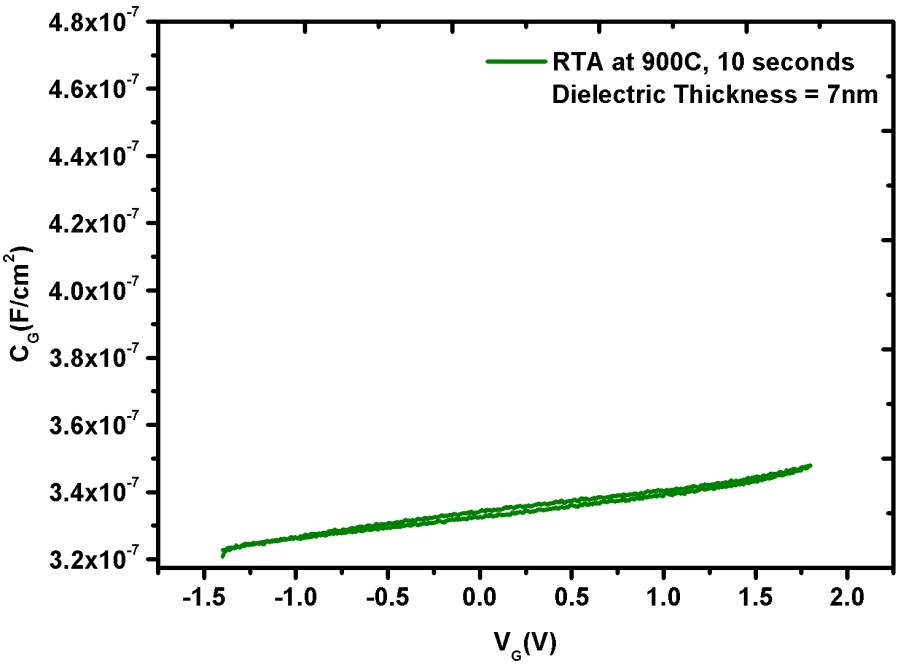

Fig 5.3.1.2.1: C-V Characteristics of RF-Sputtered AlN on SiC MIS Capacitors with RTA temperature= 900℃ and Time = 10 sec

Although the lower leakage current densities were obtained, they were larger compared to reported results, though for a thicker AlN layer [9]. Moreover, capacitance-voltage curves were also not obtained. Hence, a higher temperature and time duration of post deposition RTA is needed.

5.3.2 Rapid Thermal Annealing at 1000℃ for 120 seconds

The devices characterised in this section were exposed to RTA for 120 second (2mins) at a temperature of 1000℃. The thickness of the deposited AlN layer was found to be 7nm by measuring with ellipsometer.

5.3.2.1 Current-Voltage Characteristics

The current versus voltage plots of the RF-sputtered AlN MIS capacitors subjected to Post deposition rapid thermal annealing for 120 seconds at 1000℃ are shown in Fig 5.3.2.1.1, and the Current-density versus electric field characteristics are shown in Fig 5.3.2.1.2.

The dependence of surface leakage current on area is further less compared to Fig 5.3.1.1.2 of previous section. It has been reported that AlN undergo surface reconstruction in annealing process where the smaller grains merge to form bigger grains. AlN thin films are smooth and stable on and below the RTA temperature of 1000℃. These may mean that the defects in the layer are less, giving more uniformity and lesser leakage current densities [8].

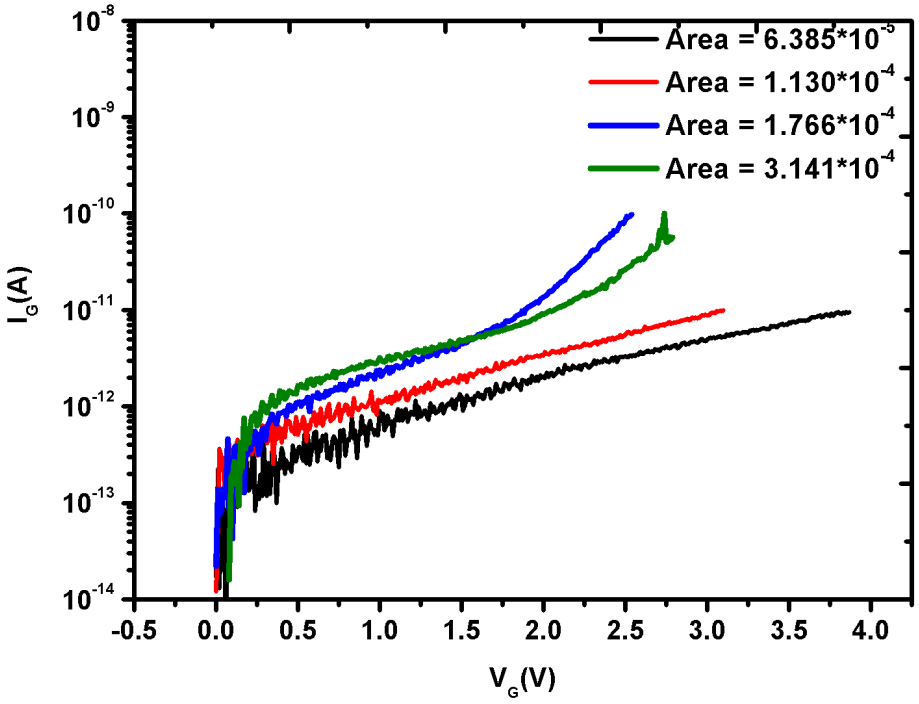

Fig 5.3.2.1.1: I-V Characteristics of RF-Sputtered AlN on SiC MIS Capacitors of different areas with RTA temperature= 1000℃ and Time = 2mins

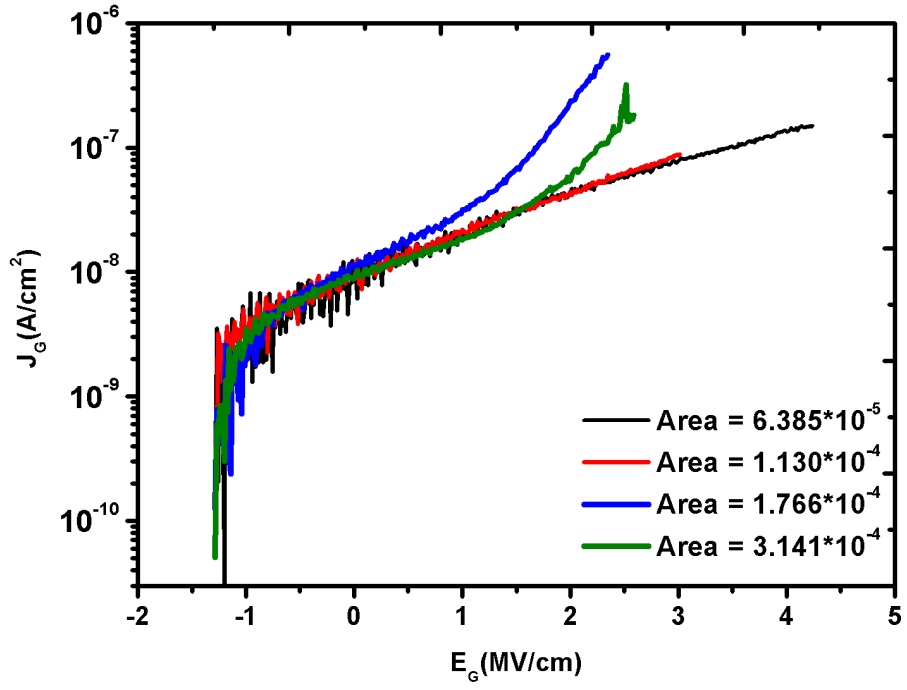

Fig 5.3.2.1.2: J-E Characteristics of RF-Sputtered AlN on SiC MIS Capacitors of different areas with RTA temperature= 1000℃ and Time = 2mins

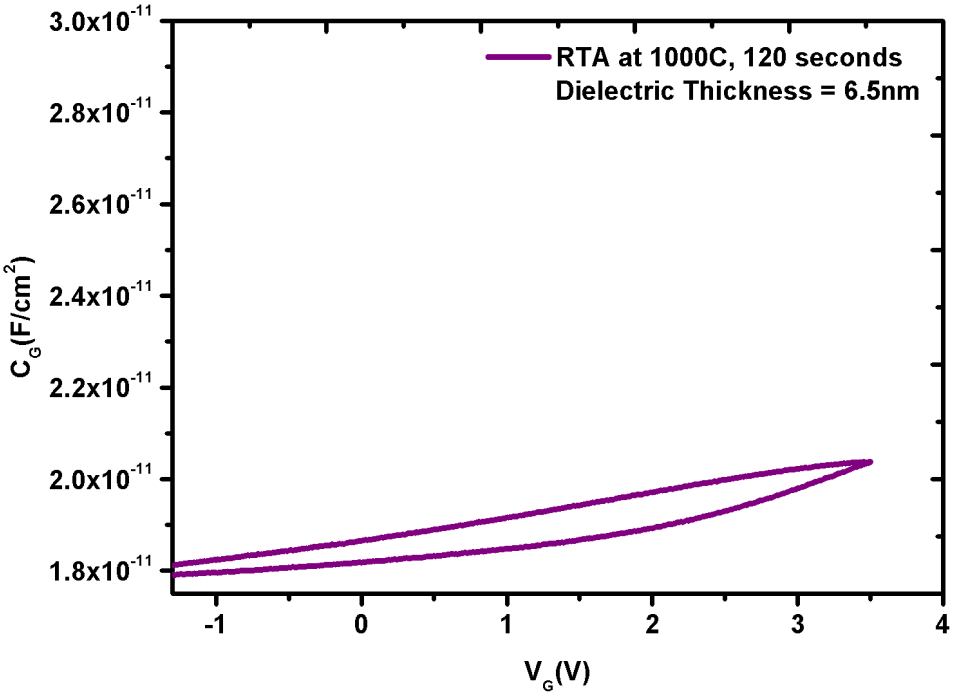

Fig 5.3.2.2.1: C-VCharacteristics of RF-Sputtered AlN on SiC MIS Capacitors with RTA temperature= 900℃ and Time = 10 sec

5.3.2.2Capacitance-Voltage Characteristics

Fig 5.3.2.2.1 shows the C-V characteristics obtained from RF-sputtered AlN MIS capacitors subjected to post deposition RTA for 120seconds at 1000℃. Again, a complete C-V curve was not obtained due to a large positive flatband voltage. Although, the MIS capacitors could be biased to higher voltages compared to Fig 5.3.1.3 because of improved breakdown field.

The increase of RTA time and temperature to 2 minutes and 1000℃ has led to lower leakage current densities around $1.803 \times 10^{-8} A/cm^2$ as compared to $4.861 \times 10^{-7} A/cm^2$ reported in the previous section 5.3.1.1 for RTA time and temperature of 10 seconds and 900℃. The MIS capacitors could be biased to higher voltages due to slight improvement in breakdown field to $3.5 MV/cm$. However, further improvement in breakdown field is desired to be able to get a C-V curve and to analyse the dielectric parameters.

5.3.3 Rapid Thermal Annealing at 1000℃ for 120 seconds with increased Dielectric Layer thickness

A better breakdown field and further reduction in current density of the AlN dielectric layer is desired. However, if the RTA temperature is further increased, it might lead to more root mean square (RMS) roughness of the AlN films [8]. Hence a higher thickness of AlN layer is opted for.

All the experimental details were the same as mentioned in section 5.2, except that the time of deposition was changed to 30mins. As a result, the thickness obtained was 14nm as measured by ellipsometer. The MIS capacitors fabricated had an area of $4.906 \times 10^{-4} cm^2$.

5.3.3.1 Current-Voltage Characteristics

For the RF-sputtered MIS capacitor with AlN layer thickness of 14nm and subjected to Post deposition rapid thermal annealing for 120 seconds at 1000℃, the current versus voltage plot is shown in Fig 5.3.3.1.1.

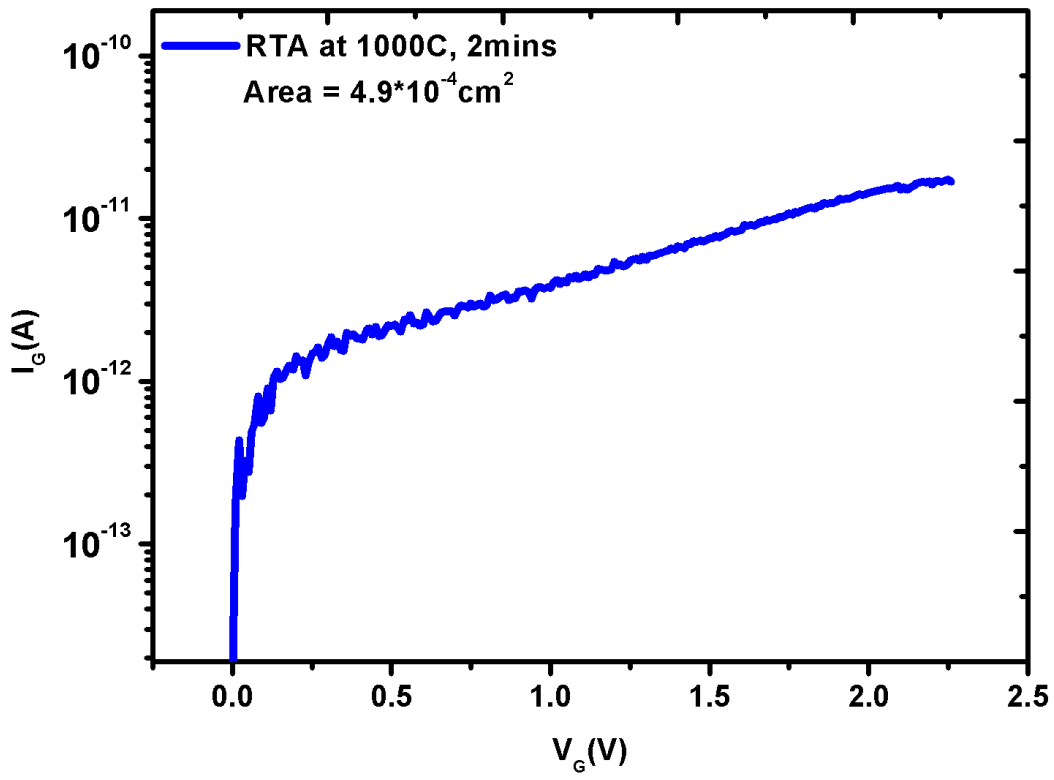

Fig 5.3.3.1.1 : I-VCharacteristics of RF-Sputtered AlN on SiC MIS Capacitors of thickness 14nm with RTA temperature= 1000℃ and Time = 2mins

The values of leakage currents have further reduced. For devices of the same area, devices with 14nm AlN layer showed a leakage current of $7.596 \times 10^{-12} A$ compared to $3.450 \times 10^{-10} A$ at a voltage of $1.5V$. The breakdown voltage increased to $5.7V$. The breakdown field was around $3.4MV/cm$.

5.3.3.2 Capacitance-Voltage Characteristics

For the RF-sputtered MIS capacitor with AlN layer thickness of 14nm and subjected to Post deposition rapid thermal annealing for 120 seconds at 1000℃, the capacitance versus voltage plot is shown in Fig 5.3.3.2.1.

Assuming the maximum capacitance as the accumulation capacitance value and using the value of the thickness measured, the value of the dielectric constant of AlN was extracted and was found to be 3.8. This is much lower compared to the expected values of around 8-10. The probable reasons may be that annealing leads to an increase in the nitrogen concentration in the layer. As a result, this may lead nitrogen interstitials, which also contributes to the increase in negative charge concentration in the insulator layer.

Using Terman's method, the value of interface state density was estimated to be around $2.909 \times 10^{12} cm^{-2} eV^{-1}$ at 0.5eV below the conduction band E_C. Fig 5.3.3.2.2 shows the D_{it} versus $E_C - E_T$ plot.

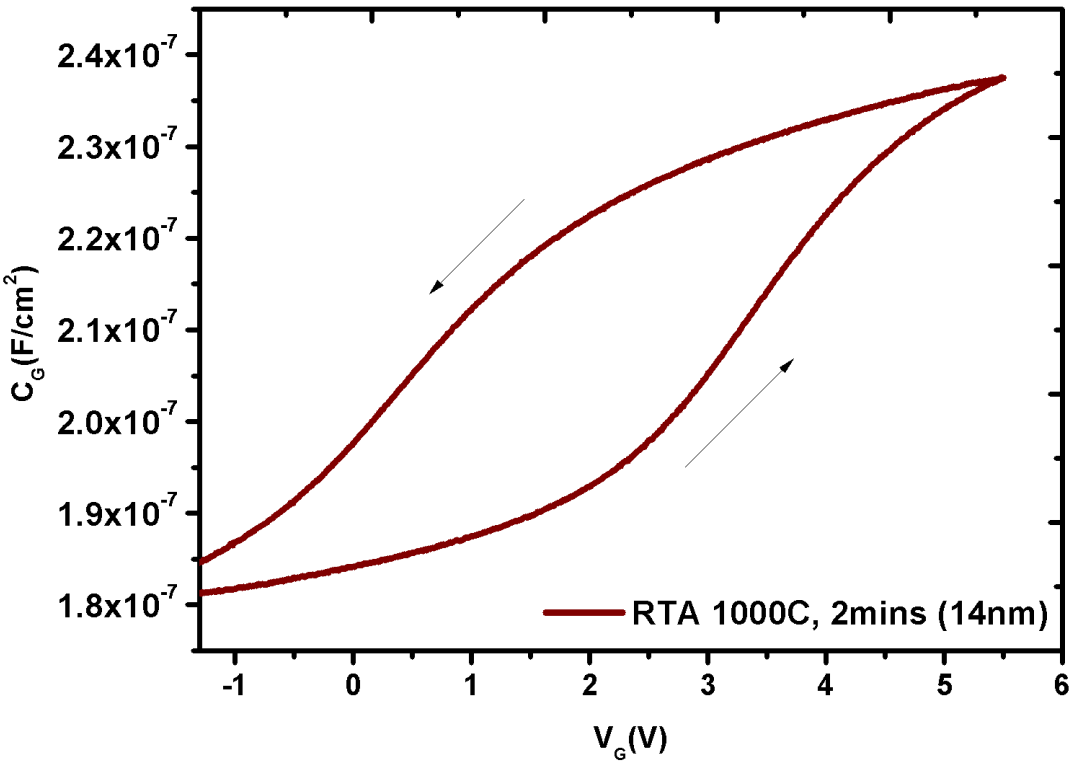

Fig 5.3.3.2.1 : C-V Characteristics of RF-Sputtered AlN on SiC MIS Capacitors of thickness 14nm with RTA temperature= 1000℃ and Time = 2mins

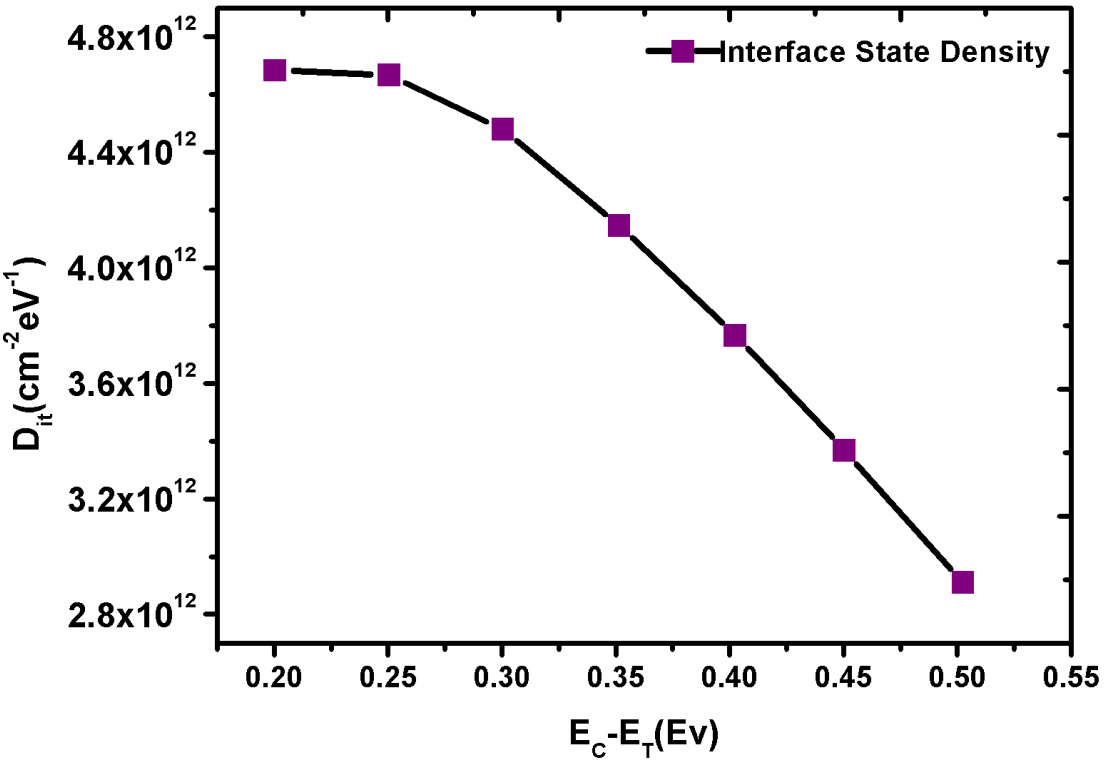

Fig 5.3.3.2.2 : Interface State Density measured using Terman's Method of RF-Sputtered AlN on SiC MIS Capacitors of thickness 14nm with RTA temperature= 1000℃ and Time = 2mins

The fixed insulator charge (Q_f) concentration is calculated to be $-3.197 \times 10^{12} cm^{-2}$ and the flatband voltage is $3.03V$. Thus, the large value of negative fixed insulator charge concentration explains the positive shift in the flatband voltage.

The C-V characteristics show a peculiar shift from the ideal C-V curve shape. This might be due to the presence of deep-level traps in the insulator layer. For obtaining the high frequency C-V curve, the voltage was swept from $-1.4V$ to $5V$ and then back to $-1.4V$. It has been reported that if the insulator layer has deep traps, the movement of electrons caused by the gate bias can lead to electrons being captured in the deep traps [23]. These electrons might move away from the interface of AlN-SiC during the holding time at $5V$. If the electrons are not release from the deep insulator traps, this causes a left-shift of the flatband voltage when the voltage is swept from $5V$ to $-1.4V$. If the MIS capacitors are biased till lower positive voltages, a lower shift in flatband voltage is observed, which is in accordance with reported results. This is shown in Fig 5.3.3.2.3

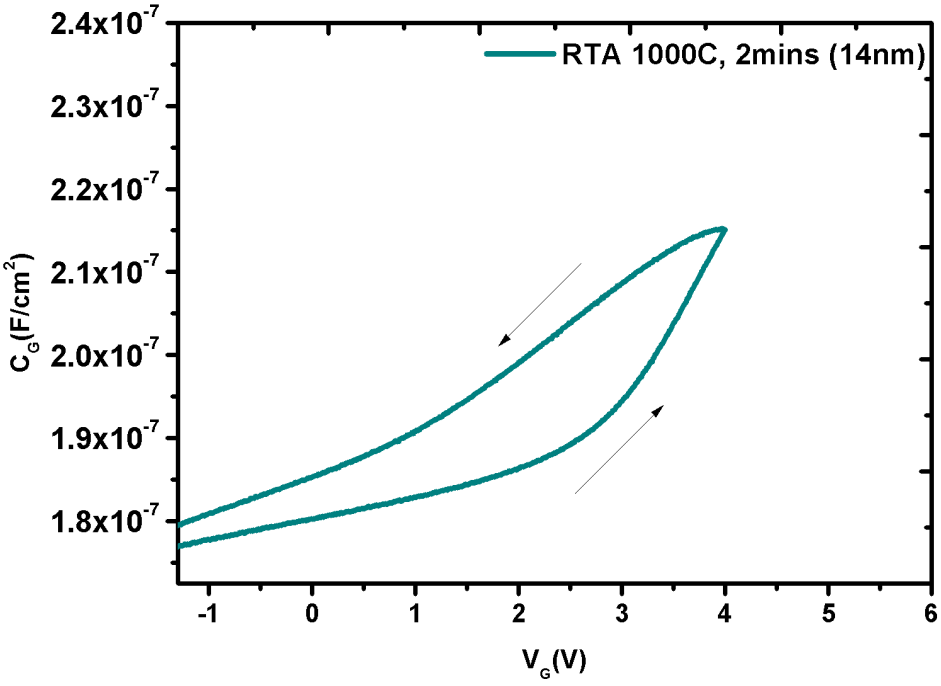

Fig 5.3.3.2.3 : C-VCharacteristics of RF-Sputtered AlN on SiC MIS Capacitors of thickness 14nm with RTA temperature= 1000℃ and Time = 2mins biased till a lower positive voltage

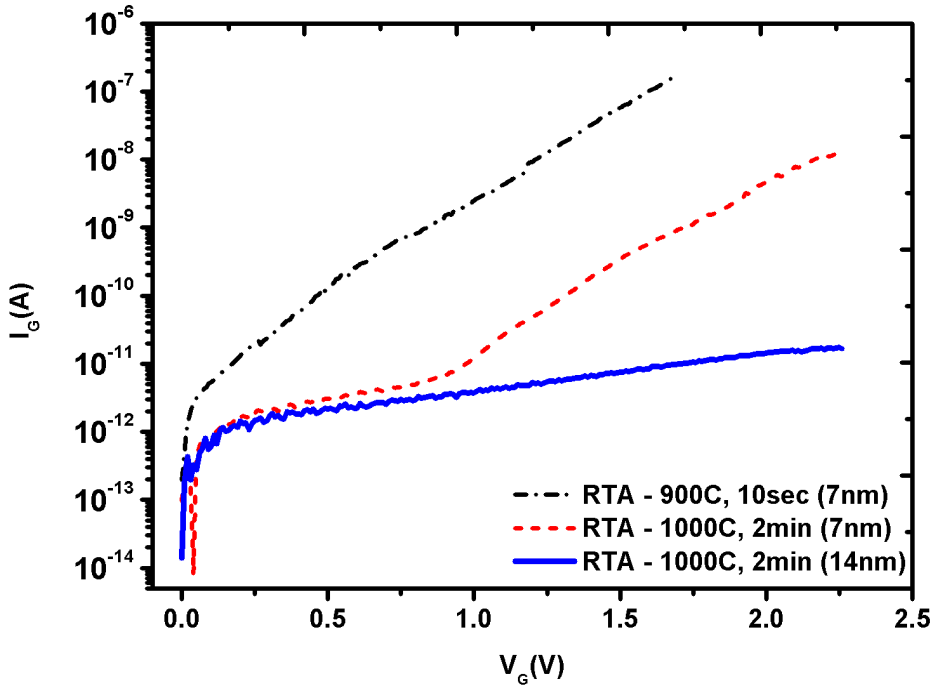

Fig 5.5.1: I-VCharacteristics of RF-Sputtered AlN on SiC MIS Capacitors of different thicknesses subjected to post deposition RTA at different temperatures (1000℃, 900℃) and Times (120sec, 10sec)

5.4 Conclusions

The RF-sputtered Al-AlN-SiC MIS capacitors were studied with respect to the effects of post deposition rapid thermal anneal with respect to time and temperature. In case of the devices with smaller thickness of 7nm, increasing the RTA temperature and time from 900℃, 10seconds to 1000℃, 120 seconds gave an improvement in the values of leakage current from $5.880 \times 10^{-8} A$ to $3.450 \times 10^{-10} A$ at a voltage of $1.5V$. Further improvement is noticed in case of a thicker dielectric layer for RTA in 1000℃, 120 seconds, which gave leakage current values of $7.596 \times 10^{-12} A$ at a voltage of $1.5V$. The results are compared in Fig 5.5.1.

The C-V curves obtained are not complete in case of AlN layer of thickness 7nm. The breakdown voltage was improved by increasing the thickness to 14nm. The MIS capacitors could be biased to higher voltages and as a result, C-V curves were obtained. The value of the dielectric constant calculated was around 3.8, which is lower probably because of nitrogen vacancies.

The hysteresis and abnormal negative shift of flatband voltage in double sweeps of C-V curves are attributed to deep level traps which capture electrons and move under the influence of bias. The shift is lower for lower voltage bias. The value of interface state density was estimated to be around $2.909 \times 10^{12} cm^{-2} eV^{-1}$ at 0.5eV below the conduction band E_C using Terman's method.

In conclusion, we can say that a high temperature and time for post deposition rapid thermal anneal is needed for obtaining lower leakage current. A thicker AlN layer if favoured for obtaining higher breakdown voltages.

CHAPTER 6

SUMMARY AND CONCLUSIONS

SiC is an attractive material for high temperature high power devices. AlN has a high dielectric constant and can provide all the advantages of being a high-k dielectric material. Its thermal conductivity is also high. Also, the lattice mismatch between AlN and SiC is reported to be low. So, AlN is a possible choice for making Al-AlN-SiC MIS capacitors.

In this study, Al-AlN-Si MIS capacitors were fabricated using RF sputtering deposition technique. The effect of nitrogen flow rate with respect to argon flow rate was studied and it was observed that a higher N_2/Ar flow rate ratio gave better leakage current and capacitance characteristics. The thickness obtained was marginally higher compared to lower flow rate ratios. Following this, the after effects of PMA was studied on the same with respect to electrical characteristics, which further confirmed that a higher N_2/Ar flow rate ratio is the most suitable parameter, with N_2 flow rate = 30sccm and Ar flow rate = 20 sccm.

Using the optimised flow rate parameters, the effects of PDA times at a particular temperature of 400℃was observed. This showed that there was improvement in electrical characteristics with increase in PDA time. The best leakage current characteristics were obtained in case of PDA time of 20 mins and 30 mins. Although the capacitance-voltage curves had a hysteresis window, the devices subjected to PDA for 30mins showed less negative flatband voltage. Following this, the combined effect of PDA and PMA was studied, which showed that post PMA, the hysteresis window reduced significantly. The overall optimised parameters for deposition and furnace annealing were summarised.

Using the optimised parameters, Al-AlN-SiC MIS capacitors were fabricated. The devices subjected to low temperature furnace-PDA showed lower leakage current densities compared to those without PDA. However, because of large positive flatband voltage shift, completer C-V curves were not obtained. Hence, post metalization anneal was carried out. Devices subjected to both PDA and PMA showed different than expected current-voltage characteristics, the reasons of which need to be investigated. But this led to an improvement of the breakdown field because of which complete C-V characteristics were obtained. A large positive flatband voltage shift was noted which was attributed to the presence of a large

concentration of negative fixed insulator charges. This was further confirmed by the Q_f estimation by Terman's method. The values of interface state density were estimated and plotted.

To improve the leakage current characteristics, rapid thermal annealing as PDA was implemented. The effects of RTA temperature and time were studied on MIS capacitors with different dielectric thicknesses. An RTA temperature and time from 900℃, 10seconds to 1000℃, 120 seconds gave an improvement in the values of leakage current. The C-V curves obtained are not complete in case of AlN layer of thickness 7nm. To further reduce the leakage current values and to improve the breakdown voltage values, a thicker AlN layer was opted. Further improvement is noticed in case of a thicker dielectric layer of 14nm for RTA in 1000℃, 120 seconds. The breakdown voltage improved as well. As result, C-V curves were obtained as the MIS capacitors could be biased to higher positive voltages. The values of fixed insulator charge concentration and interface state density were analysed from the C-V curves using Terman's method.

Thus, in this study, the parameters of AlN deposition on 4H-SiC using RF-sputtering are optimised. The effects of low temperature furnace anneal is studied both in case of post deposition annealing and post metalization annealing. Annealing helps in lowering the leakage current value. Implementing both PDA and PMA helps in obtaining good C-V characteristics. The use of rapid thermal anneal is helpful in obtaining the lowest leakage current densities.

Scope of Future Work: In this study RTA is used in nitrogen ambient. Although low values of leakage currents were obtained, the C-V curves had a distorted shape and large hysteresis. The reason is most likely to be the high interface density state. The dielectric constant of AlN extracted is lower than expected. It would be interesting if studies are done to reduce the effect of hysteresis and the high interface density state. Also, other parameters for RTA time and temperature could be studied for higher AlN layer thickness in order to obtain higher breakdown field. If complete and ideal capacitance characteristic are obtained and a dielectric constant closer to ideal is achieved, further studies can aim to investigate the leakage current mechanisms in Al-AlN-SiC MIS capacitors in higher temperatures.

REFERENCES

[1] Jayant Baligaa, “Silicon Carbide Power Devices”, 2005

[2] Divya Kurthakoti Chandrashekhara**, “**“Future Transportation Power Electronics: Wide Bandgap Devices”, URL: http://electricvehicle.ieee.org/2014/10/31/future-transportation-power-electronics-wideband-gap-devices/

[3] Burak Ozpeneci, Madhu Sudhan Chintavali, Leon M. Tolbert, “Enhancing power electronic device with wide bandgap semiconductors”,

URL: (http://web.ornl.gov/info/ornlreview/v40_2_07/2007_msc_enhancing_pwr.pdf)

[4] R. H. Dennard, Gaenssle. Fh, H. H. Yu, V. L. Rideout, E. Bassous, and A. R. Leblanc, “Design of Ion-Implanted MOSFETS with Very Small Physical Dimensions”, IEEE Journal of Solid-State Circuits, vol. SC 9, pp. 256-268, 1974

[5] G. E. Moore, “Cramming more components onto integrated circuits”, Proceedings of the IEEE, vol. 86, pp. 82-85, Jan 1998

[6] International Technology Roadmap for Semiconductor, Semiconductor Industry Association 2008 edition, December 2008

[7] Eliso Ruiz an Santiago Alvarez, “Electronic structure and Properties of AlN”, Physical Reviw B, Volume 49, Number 11, 15 March 1994-I

[8] B. Liu, J. Gao, K.M. Wu, C. Liu, “Preparation and rapid thermal annealing of AlN thin films grown by molecular beam epitaxy”, Solid State Communications, Volume 149, Issues 17–18, May 2009, Pages 715–717

[9] Kwang-Ho Kim, Yong-Seong Kim, Sang-Hyun Jeong and Soon-Won Jung, “Fabrication and Properties of an Epitaxial AlN Film on a SiC Substrate by Using RF Magnetron Sputtering”, Journal of the Korean Physical Society, Vol 48, No. 2, February 2006, 275-278

[10] J.P. Kar, G. Bose, S. Tuli, “Influence of rapid thermal annealing on morphological and electrical properties of RF sputtered AlN films”, Materials Science in Semiconductor Processing, Volume 8, Issue 6, 2005, Pages 646–651

[11] V. Dimitrova a, D. Manova, E. Valcheva, “Optical and dielectric properties of dc magnetron sputtered AlN thin films correlated with deposition conditions”, Materials Science and Engineering B68 (1999) 1–4

[12] J. Fan and P.K. Chu, “General Properties of Bulk SiC”, Chapter 2 – ‘Silicon Carbide Nanostructures’, Engineering Materials and Processes 2014, pp 7-114

[13] F Litimein, B Bouhafs, Z Dridi1, and P Ruterana, “The electronic structure of wurtzite and zincblende AlN: an ab initio comparative study”, New Journal of Physics 4 (2002) 64.1–64.12

[14] Z.X. Bi, Y.D. Zhang, S.L. Hu, X.Q. Xiu, L.L. Zhou, B. Shen, D.J. Chen, Y. Shi, “Dielectric Properties of AlN film on Si substrate”, Journal of Materials Science: Materials in Electronics 15(2004) 317-320

[15] S. Simeonovi, S. Bakalova, E. Kafedjiiskai, A. Szekeresi, S. Grigorescu, F. Sima, G. Socol, I.N. Mihailescu, “Al/AlN/Si MIS Structures with Pulsed-Laser-Deposited AlN Films as Gate Dielectrics: Electrical Properties”, Romanian Journal of Information Science and Technology, Volume 10, Number 3, 2007, 251–259

[16] T. Adam, J. Kolodzey, C.P. Swann, M.W. Tsao, J.F. Rabolt, “The electrical properties of MIS capacitors with AlN gate dielectrics”, Applied Surface Science 175-176 (2001) 428-435

[17] URL:

http://www.engr.sjsu.edu/sgleixner/mate129/Continuing%20Ed/Deposition/sputtering.pdf

[18] URL: http://reactive-sputtering.info/node/99

[19] URL: http://users.wfu.edu/ucerkb/Nan242/L08-Sputtering_b.pdf

[20] URL: http://www.kfupm.edu.sa/sites/tsf/AnalyticsReports/sputtering.pdf

[21] Jyoti Prakash Kar and Gouranga Bose, “Aluminum Nitride (AlN) Film Based Acoustic Devices: Material Synthesis and Device Fabrication”, Acoustic Waves – From Microdevices to Helioseismology, Chapter 25

[22] URL: http://www.ag-rtp.com/rapid-thermal-process-2.htm

[23] Javed Karamdel, C.F. Dee, M.M. Salleh, Burhanuddin Y.M., “Characterization of Aluminium Nitride Nano Film Deposited by RF Magnetron Sputtering in Buffer Layer Applications”, World Applied Sciences Journal 9 (Special Issue of Nanotechnology): 52-55, 2010, ISSN 1818-4952

[24] V. VasanthiPillay, K. Vijayalakshmi, “Influence of Sputter Deposition Time on the Growth of c-Axis Oriented AlN/Si Thin Films for Microelectronic Application”, Journal of Minerals and Materials Characterization and Engineering, 2012, 11, 724-729

[25] Jae-Seung Choi, Weoun-Seon Lee, Dong-Hyun Shin, Hyun-Gyoo Lee, Yeong-Seuk Kim and Keun-Hyung Park, “Abnormal Hysteresis Property of SiC Oxide C-V Characterisics”, Materials Science Forum Vols. 389-393 (2002) pp 1021-1024

[26] Jerry L. Hudgins, Grigory S. Simin, Enrico Santi, M. Asif Khan, “An Assessment of Wide Bandgap Semiconductors for Power Devices”, IEEE TRANSACTIONS ON POWER ELECTRONICS, VOL. 18, NO. 3, MAY 2003